Review Article

Strength and Chemical Characterization of Ultra High-Performance Geopolymer Concrete: A Coherent Evaluation

Midhin A. K. Midhin [1, 2], Leong Sing Wong [1, 2*], Ali Najah Ahmed [1, 2],
Al Mashhadani D. A. Jasim [1, 2], Suvash C. Paul [3]

[1] Department of Civil Engineering, College of Engineering, Universiti Tenaga Nasional, Jalan IKRAM-UNITEN, 43000 Kajang, Selangor, Malaysia.

[2] Institute of Energy Infrastructure, Universiti Tenaga Nasional, Jalan IKRAM-UNITEN, 43000 Kajang, Selangor, Malaysia.

[3] Department of Civil Engineering, International University of Business Agriculture and Technology, Dhaka 1230, Bangladesh.

Abstract

The objective of this review article is to analyze published data encompassing compressive strength, tensile strength, elastic modulus, and flexural strength, as well as the utilization of scanning electron microscopy (SEM), energy dispersive x-ray spectroscopy (EDS), and x-ray diffraction (XRD) for Ultra High-Performance Geopolymer Concrete (UHP-GC), with the focus of establishing the current research trends regarding its mechanical, microstructural, and chemical characteristics. After a critical evaluation of the published data from the literature findings, it became evident that UHP-GC can attain a remarkably high level of engineering performance. In UHP-GC, the optimum percentage of silica fume as a slag partial replacement to achieve high compression, tensile, and elastic modulus were traced to be 25, 30, and 35%, respectively. The optimum ratio of sodium silicate to sodium hydroxide and sodium hydroxide molarity for UHP-GC were identified to be 3.5 and 16, respectively. All in all, the review provides a thorough understanding of the review gap and distinct functions of different raw materials in decreasing porosity and enhancing the formation of geopolymeric gels that not only bond but also strengthen UHP-GC. UHP-GC stands as an energy-saving material in concrete technology, poised to forge a path towards a sustainable future for the building sector.

Keywords: Ultra High-Performance Geopolymer Concrete; Mechanical; Microstructural; Chemical; Raw Materials; Energy-Saving.

1. Introduction

Concrete stands as the prevailing choice for construction, widely adopted across various projects. However, it is crucial to note that the production of each ton of Ordinary Portland Cement (OPC) necessitates approximately 1.5 tons of raw materials, leading to significant carbon dioxide (CO_2) emissions being released into the atmosphere [1, 2]. Geopolymer concrete (GPC) has emerged as a viable alternative to reduce the environmental problems caused by OPC concrete. Other than the aggregates, part of the GPC is normally composed of fine silica and alumina-based raw materials such as metakaolin [3, 4] or industrial waste such as fly ash [5, 6] and ground granulated blast furnace slag (GGBS) [7, 8], which are then activated with an alkaline activator solution (AAS) such as sodium hydroxide (NaOH) or potassium hydroxide (KOH) in combination with sodium silicate (Na_2SiO_3) [9–11]. Much of the literature on concrete characterization has focused on the partial incorporation of cement with aluminosilicate elements. In recent years, research has focused on replacing OPC with more environmentally friendly cement for the long-term durability of cement composites [12–14].

UHP-GC is a strong concrete material that can be researched and explored in a sustainable manner. Research on UHP-GC is motivated by the need to achieve the United Nations 12th Sustainable Development Goal, which is 'Responsible Consumption and Production'. The aim is to reduce waste generation by recycling the waste materials used in the production of UHP-GC. UHP-GC offers a greener option to OPC concrete, as it eliminates the need for Portland cement while still ensuring exceptional durability. UHP-GC has an impressively high compressive strength of over 150 MPa, which makes it exceptionally durable, strong, and resistant to environmental damage [15]. Its robust condition stems from the remarkable efficiency of packing, a direct consequence of the strong geopolymeric bonding present in UHP-GC. This bonding primarily comprises inorganic components, often ceramic aluminosilicates, which intricately form extensive networks bonded through covalent interactions. Remarkably, these networks exhibit a non-crystalline (amorphous) and semi-crystalline nature. One key advantage of UHP-GC production is that it is a green method for creating durable materials that can be used in various applications. Ambily et al. [16] showed that when slag and silica fume are used as precursors in geopolymerization, UHP-GC could achieve a compressive strength of 175 MPa. To produce standard UHP-GPC, several key methods can be employed. These include implementing curing processes in a pressurized environment or through heating, incorporating a mixture of Ground Granulated Blast Furnace Slag (GGBS) and silica fume (SF) to enhance flowability, and promoting efficient activation of alkalis at lower precursor-to-water ratios. Moreover, efforts can be made to augment the specific surface area and reduce the size of precursor particles while utilizing alkaline solution-based potassium as the activator. The advantages of adopting UHP-GC go beyond its exceptional strength and durability. Construction organizations may reduce their environmental impact while maintaining high-quality construction requirements by switching to UHP-GC. For that reason, it is a viable alternative to standard Portland cement-based concrete due to its excellent compressive strength, eco-friendliness, and potential for lowering carbon emissions.

The properties of UHP-GC are engineered to achieve a very high level of toughness and endurance, making it a possible solution for a variety of infrastructure issues. Due to its stronger chemical bonding, UHP-GC demonstrated better resiliency than normal concrete to fend off harsh environments. In terms of mechanical characteristics, it is evident that UHP-GC is superior to normal concrete. Although UHP-GC has not been extensively investigated, it is recognized that due to its stronger chemical composition, it would have even better mechanical properties, and more research work needs to be carried out to prove it. Furthermore, the improved mechanical characteristics of UHP-GC might have significant benefits in a variety of infrastructure applications. It can, for example, increase the durability of buildings, bridges, and offshore platforms. UHP-GC can also contribute to lower long-term maintenance costs since it can endure natural catastrophes and corrosive conditions [17–25]. With the intensification of research and commercialization efforts, there is growing anticipation for the widespread adoption of UHP-GC within the building sector. As its potential continues to be explored, UHP-GC is poised to become increasingly prevalent in construction practices. This article provides a coherent overview of the engineering properties of UHP-GC.

Until recently, there were only a limited number of review articles focused on the engineering and durability assessment of UHP-GC. Samuvel Raj et al. [26] and Dheyaaldin et al. [27] reviewed the impact of nanomaterials on the mechanical and durability properties of geopolymer concrete. Although nanomaterials like nano-silica and nano-clay are recognized for their large surface areas and high reactivity in geopolymerization, their potential to enhance the performance of geopolymer concrete has not been comprehensively appraised in these reviews. In a separate review conducted by Qaidi et al. [24], a comprehensive evaluation of the technical and production aspects of recent advancements in UHP-GC was presented. This encompassed consideration of environmental factors, mix design, fresh properties, mechanical properties, dynamic behavior, strain hardening, durability features, microstructural properties, as well as the relationship between compressive strength, splitting tensile strength, and modules of elasticity. The review did not thoroughly examine and compare the bonding mechanisms in geopolymerization relevant to UHP-GC using different precursors and fibers. Furthermore, Swathi & Vidjeapriya [28] did a review comparing the fresh, mechanical, and durability characteristics of normal-strength geopolymer concrete, high-performance geopolymer concrete, and UHP-GC. However, the review did not establish direct correlations between the properties of UHP-GC and their microstructures and chemical characteristics in a comprehensive manner. From these observations, it is evident that there exists a gap in the review concerning the influence of various precursor types and fibers on the engineering behavior of UHP-GC and the roles these materials play in the geopolymerization behavior of UHP-GC.

To close the review gap, it is pertinent to assess the outcomes of the recently published articles on UHP-GC, which was meticulously established to exhibit exceptional toughness and durability, thus proving it to be a promising solution for a wide range of infrastructure challenges. The choice to review the strength and chemical characteristics of UHP-GC is grounded in the necessity for a thorough analysis of the existing literature, which can yield valuable insights into the resilience of UHP-GC, an attribute directly influenced by its mineralogical composition and mixture components. The chemical reactions initiated by various types of precursors in the presence of an alkaline activator during geopolymerization play a pivotal role in determining the bonding mechanism and the robustness of UHP-GC. Considering these facts, this review article is designed with the objective of providing a comprehensive evaluation of the strength and chemical properties of UHP-GC based on the relevant published articles. The review analysis of the UHP-GC formulation aimed to elucidate the functions performed by various raw materials, shedding light on their

potential to bolster toughness and reinforcement. Besides, the analysis in this review focuses on the specific effects of alkaline activation and varying concentrations of sodium hydroxide on the bonding properties of UHP-GC. The microscopic images and chemical compositions of UHP-GC are then corroborated to back up the literature findings on the superior mechanical performance of UHP-GC. The flowchart that illustrates the method of the review is shown in Figure 1.
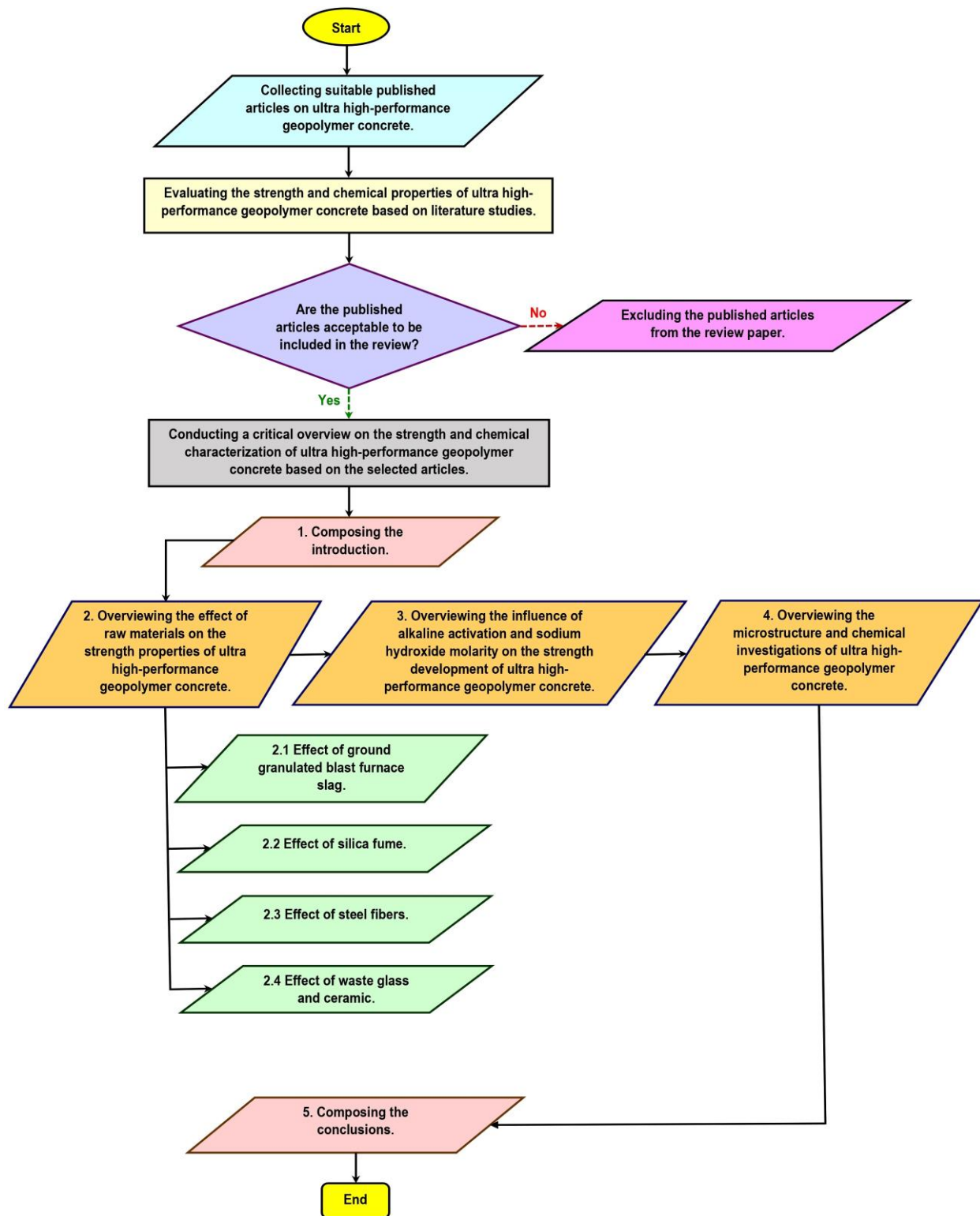
Figure 1. Flowchart that illustrates the method of the review

2. Effect of Raw materials on the Strength Properties of UHP-GC

The impact of raw materials on the strength characteristics of Ultra High-Performance Geopolymer Concrete (UHP-GC) is comprehensively reviewed in Section 2. The compressive strength and elastic modulus development

of UHP-GC enhanced using various raw materials are elucidated in detail, with a focus on its optimal performance. The factors that influenced the raw materials for improving the toughness of the UHP-GC are specifically highlighted.

2.1. Effect of Ground Granulated Blast Furnace Slag

GGBS was used as a precursor for geopolymerization in UHP-GC in the published study of Lao et al. [29]. GGBS, an essential component in construction materials, is derived from the rapid cooling of molten iron slag produced during the iron and steel-making process. This cooling method utilizes water or steam quenching, transforming the slag into a finely powdered product with a granular and glassy texture after drying. GGBS applied in concrete has a high content of silica ($SiO_2 = 30\%$) and calcium oxide ($CaO = 46.5\%$). Other than GGBS, coal fly ash was used as a precursor of UHP-GC under the study. With a particle size of 300 μm, the fine silica sand was applied as the fine aggregate for the concrete. The alkaline activator solution was produced from a mixture of anhydrous sodium metasilicate (Na_2SiO_3) and water glass. In the study, the mix designs of the concrete were varied with water to precursor (w/p) ratios ranging from 0.22 to 0.27 and fly ash to GGBS (FA/GGBS) ratios of 0.25, 1, and 4. With the mix designs set at a w/p ratio of 0.27 and the FA/GGBS ratio reduced from 4 to 0.25, the concrete's compressive strength improved from 94.4 to 156.9 MPa. Other than that, by setting the mix designs at a w/p ratio of 0.22 and the FA/GGBS ratio reduced from 4 to 0.25, the concrete's compressive strength improved from 103.9 to 180.7 MPa (Figure 2). The literature findings revealed that an optimal w/p ratio and a reduced FA/GGBS ratio had a positive influence on the strength enhancement of the UHP-GC.

Reducing the FA/GGBS ratio in the concrete implies more calcium sources were available for alkaline activation, resulting in increased hardening. Figure 3 illustrates the ultimate tensile strength of UHP-GC at varying w/p and FA/GGBS ratios. It is evident from the figure that by fixing the mix designs at a w/p ratio of 0.27 and decreasing the FA/GGBS ratio from 4 to 0.25, the ultimate tensile strength of the concrete increased from 11.2 to 12 MPa. When the w/p ratio was set at 0.22 and the FA/GGBS ratio was decreased from 4 to 0.25 in the mix designs, the ultimate tensile strength of the concrete increased from 14.5 to 15.9 MPa. The trend of increase in the ultimate tensile strength of the concrete is the same as that of its compressive strength. The increase in GGBS content in the geopolymer concrete admixtures probably increased the pH, resulting in optimizing the concrete's alkaline reactivity, which enhanced its geopolymerization process. This is attributed to the greater calcium oxide and alumina compositions in GGBS than those of FA, which led to the development of more geopolymeric gels that further strengthened the UHP-GC.
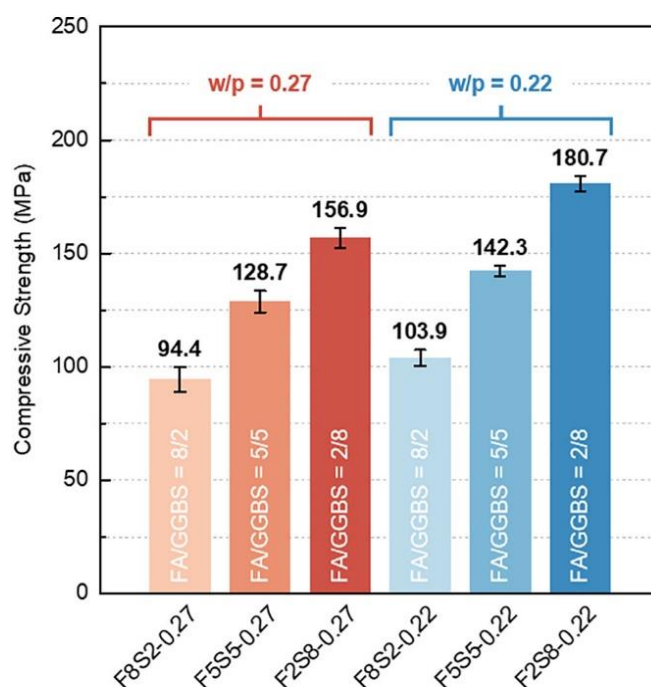
Figure 2. Influence of ground granulated blast furnace slag and fly ash on the compressive strength of ultra high-performance geopolymer concrete [29]
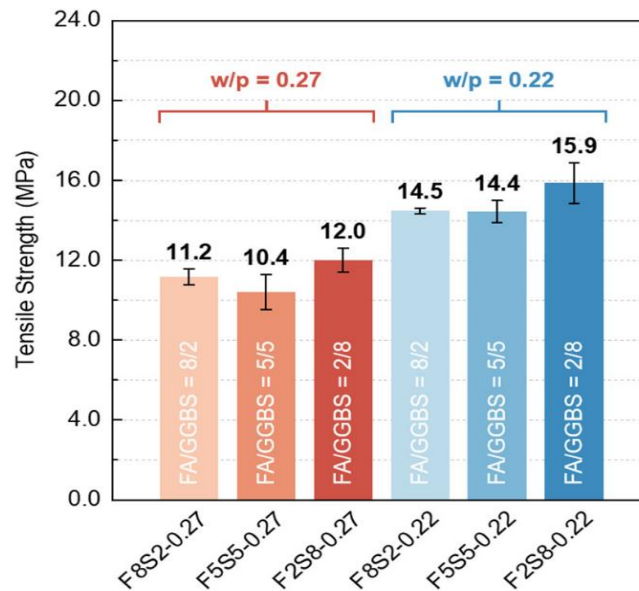
Figure 3. Influence of ground granulated blast furnace slag and fly ash on the tensile strength of ultra high-performance geopolymer concrete [29]

2.2. Effect of Silica Fume

Silica fume is a byproduct of the manufacturing of ferrosilicon alloys that have a particle size of less than 1μm [30]. It has the capability to strengthen UHP-GC by participating as a precursor in geopolymerization and acting as a filler that increases its compactness and reduces its voids and water absorptivity. Liu et al. [23] tested the compressive strength and elastic modulus of UHP-GC specimens, which contain a high dosage of fly ash and GGBS with varying ratios of silica fume (5, 10, 20, and 30%) of the total binder volume. The UHP-GC specimens were subjected to standard curing at room temperature. The compression test results are presented in Figure 4. Both the compressive strength and elastic modulus of the concrete specimens were recorded to be over 150 MPa and 32 GPa, respectively. It is observable from Figure 4 that there were drastic reductions in the compressive strength and elastic modulus values of the concrete with increasing silica fume concentrations from 5 to 10%. Beyond the 10% dosage of silica fume in the UHP-GC specimens, the compressive strength value increased progressively. The trend implies that there is a possible improvement in the compressive strength of the concrete specimens beyond a silica fume dosage of 30%. Such an occurrence is probably due to the very fine particles in silica fume that not only induced the formation of geopolymeric gels in the concrete but also intensified its bonding action.
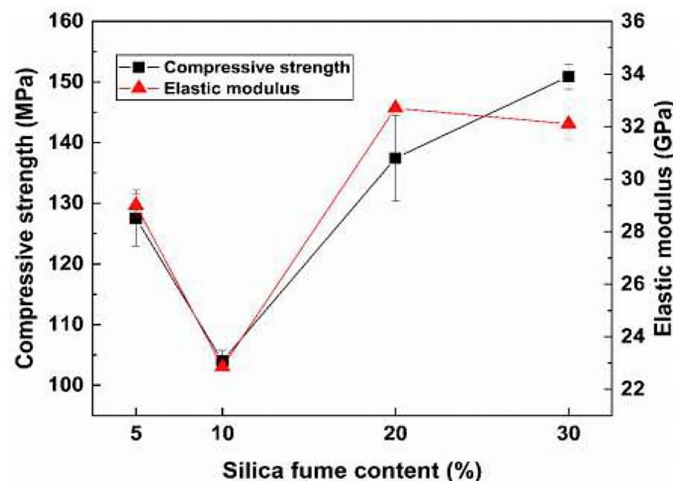
Figure 4. Ultra high-performance concrete's compressive strength and elastic modulus with varying concentrations of silica fume [23]

The effect of micro silica (also known as silica fume) on the mechanical characteristics of UHP-GC was also investigated by Aisheh et al. [31]. Fly ash, GGBS, and micro silica were applied as the precursors for developing the UHP-GC specimens. The micro silica content in the mix designs of the concrete specimens varied by 5, 10, 15, and 25% based on the total mass of the binder utilized. The impact of the micro silica compositions on the compressive strength

and elastic modulus of the UHP-GC specimens is depicted in Figure 5. There were positive changes in the compressive strength and elastic modulus with the optimization of micro silica in the concrete. With 5% micro silica in the mix design, the concrete was tested and obtained a compressive strength and an elastic modulus of 128 MPa and 30 GPa, respectively. The values of the two parameters for the concrete specimen with 10% micro silica declined by 19% and 22%, respectively. A progressive improvement in the compressive strength and elastic modulus of the concrete could be observed in the results of the concrete compression tests with the mix designs having 15 and 25% micro silica. The greatest value of compressive strength was recorded from the compression test result of the concrete specimen with 25% micro silica. On the other hand, geopolymer concrete specimens with 15% micro silica have the highest modulus of elasticity. The results confirmed that the concrete's elastic modulus is not directly correlated to its compressive strength. Its stiffness is dependent on its composition, which varies over a range of micro silica percentages in the concrete.

(a)

(b)
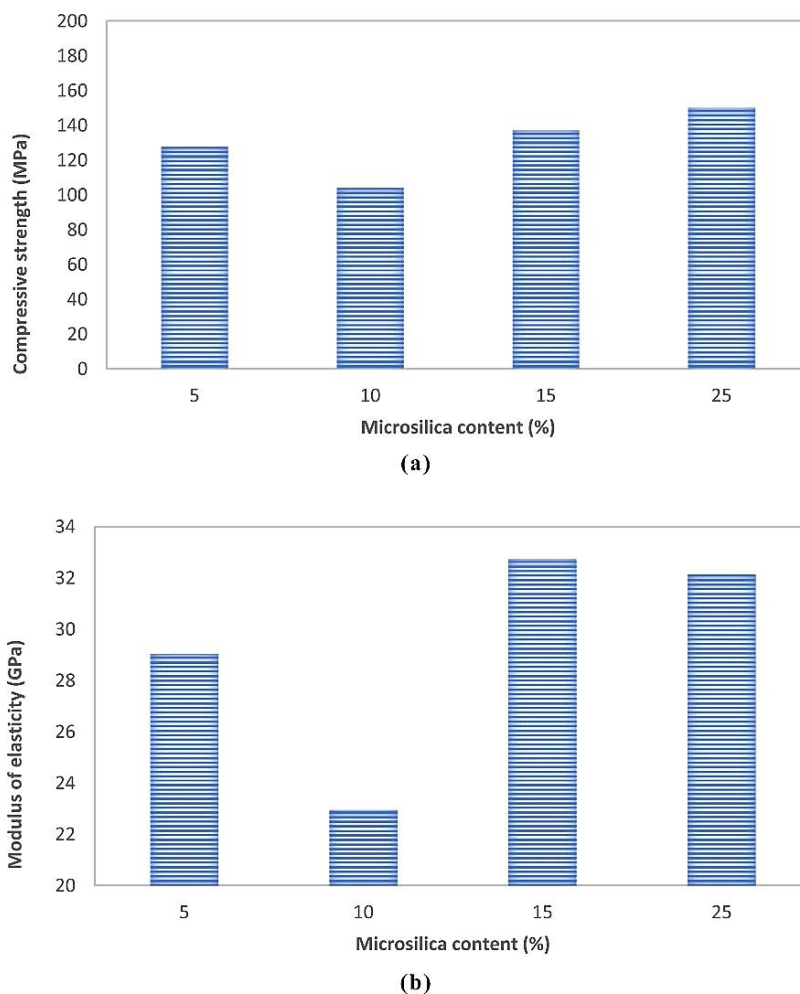
Figure 5. Relationship between micro silica dosage and (a) compressive and (b) modulus of elasticity of ultra high-performance concrete [31]

In another published work, Tayeh et al. [32] researched the strength properties of UHP-GC specimens improved with micro silica. The UHP-GC specimens were produced by incorporating GGBS, fly ash, and micro silica as the precursors. Five dosages of micro silica (0, 7.5, 15, 25, and 35%) by the total mass of the binder content were applied in the admixtures of the geopolymer concrete. The lowest compressive strength and elastic modulus were observed from the results of the geopolymer concrete with 15% silica fume, shown in Figure 6. This implies that an addition of 15% micro silica yielded the least bonding effect in the geopolymerization of the concrete. On the other hand, the geopolymer concrete with a 35% micro silica dosage had the greatest compressive strength and elastic modulus. This improvement is attributable to the effective surface area and activity of micro silica, thereby accelerating the rate at which reactive silica enters the geopolymerization process with the alkaline activator for forming strong geopolymer concrete. For the geopolymer concrete specimens with micro silica contents of 25 and 35%, there was a small difference between the values of their elastic modulus. The research findings conclusively demonstrate that the optimal mix design for geopolymer concrete, aiming for the highest compressive strength and elastic modulus, heavily relies on the synergistic effect of the combined precursors such as GGBS, fly ash, and micro silica.

(a)

(b)
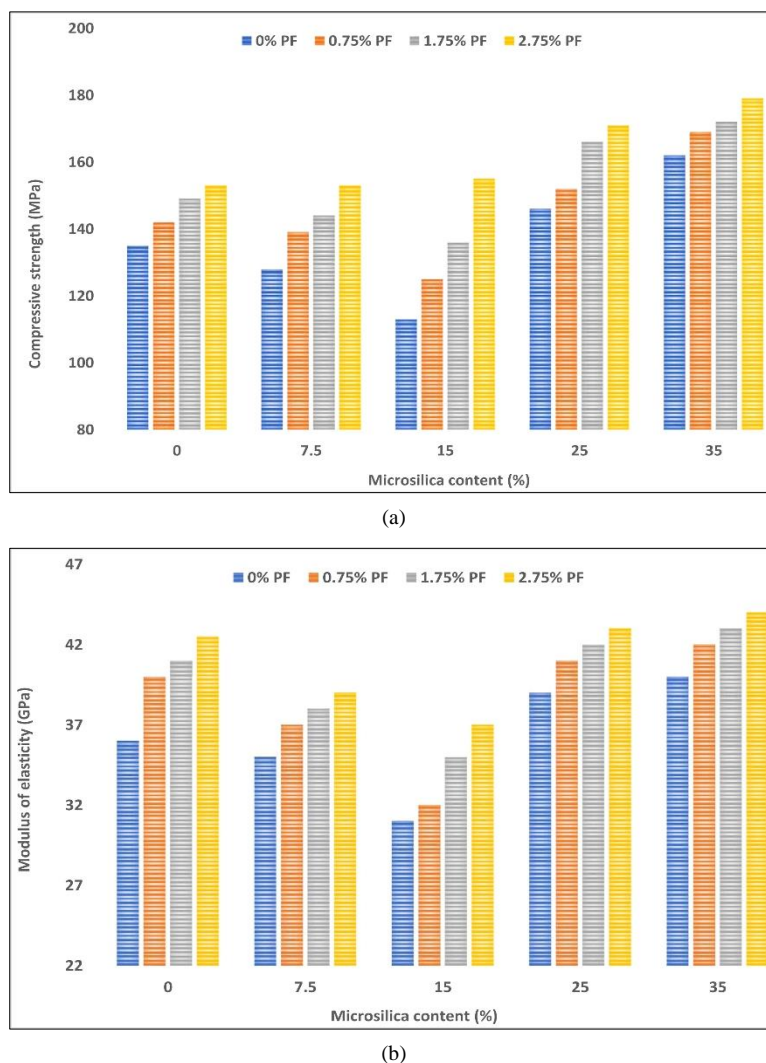
Figure 6. Relationship between micro silica and polypropylene fiber contents and (a) compressive and (b) modulus of elasticity of ultra high-performance geopolymer concrete [32]

In another study, Tahwia et al. [33] investigated the properties of UHP-GC with silica fume as partial replacements for slag at 10, 20, and 25%. The least compressive strength values of UHP-GC specimens after 28 days of curing varied from 91 to 123 MPa for the concrete mix design with a 10% silica fume dosage. However, UHP-GC specimens with a 25% silica fume dosage had a higher range of compressive strength, which varies from 124 to 152 MPa. The presence of more reactive microparticles from silica fume that effectively interact with the calcium source from GGBS and the alkaline activator to generate strong geopolymeric bonding in the concrete specimens was responsible for the increase in the compressive strength values. The lower compressive strength values of the UHP-GC specimens containing 10% silica fume were caused by a lack of reactive micro silica that could enter the geopolymeric process to yield ultra-high-strength geopolymer concrete [1, 14, 34]. Wang et al. [35] analyzed the impact of silica fume on the characteristics of UHP-GC with other concrete materials such as Class F fly ash and calcium aluminate cement (CAC). The dosages of silica fume in the concrete varied between 5 to 30% of the total binder volume. From the result analysis, it was revealed that there was a progressive enhancement in the compressive strength with the increasing dosage of silica fume for the concrete specimens with a mix design of 20% CAC. However, there was a drop in the value of the compressive strength with silica fume dosages greater than 10% for the concrete specimens with a 10% CAC mix design. The findings indicated that the ideal content of silica fume in the UHP-GC mix design is governed by the degree of alkalinity of the concrete admixture.

Kathirvel & Sreekumaran [36] developed UHP-GC based on the concept of reactive powder concrete. The objective of their research was to eliminate the use of Portland cement by blending GGBS and silica fume with an alkaline activator composed of sodium hydroxide and sodium silicate solution. Additionally, steel fibers were incorporated into the UHP-GC at dosages of 0, 1, and 2%. The silica fume content in the UHP-GC mix designs varied at 0, 142.5, and 285 kg m^{-3}. This means that silica fume was added at 0, 15, and 30% by weight of GGBS in the UHP-GC. Furthermore, the quartz content in the UHP-GC mix designs was adjusted to 20, 30, and 40%. Figure 7 illustrates the results of the 7-day and 28-day compressive strength values of UHP-GC specimens with varying dosages of silica fume and quartz. It is evident

from the published work that the compressive strength of the UHP-GC specimens increased with higher silica fume content, irrespective of the quantity of quartz and steel fibers used. For instance, when UHP-GC contained 20% quartz powder, the 28-day compressive strength increased by 13.83 and 33.66% for specimens with 15 and 30% silica fume content, respectively, compared to those without silica fume (Figure 7-a). Similarly, when the UHP-GC contained 30% quartz powder, the compressive strength results were 20.26 and 34.62% higher for specimens with 15 and 30% silica fume content, respectively, compared to those without silica fume (Figure 7-b). Additionally, for the UHP-GC with 40% quartz powder, the compressive strength was found to be 15.15 and 30.54% higher for specimens with 15 and 30% silica fume content, respectively, compared to those without silica fume (Figure 7-c). The primary reason behind the improved compressive strength resulting from higher silica fume content is its ability to fill space, creating a more compact microstructure. This reduces the need for additional water during hydration and confines the area available for fresh hydrate formation. The enhancement in compressive strength observed when incorporating silica fume is attributed to its superior surface area-to-mass ratio compared to GGBS. This characteristic leads to a higher packing density, resulting in increased strength. However, when the silica fume content reaches higher dosages (30%), the increased water demand poses a challenge as some portions of silica fume may remain unreacted in the UHP-GC. This, in turn, leads to increased heterogeneity in the UHP-GC specimens, resulting in slower compressive strength growth due to the presence of a partially weakened microstructure.

(a)

(b)

(c)
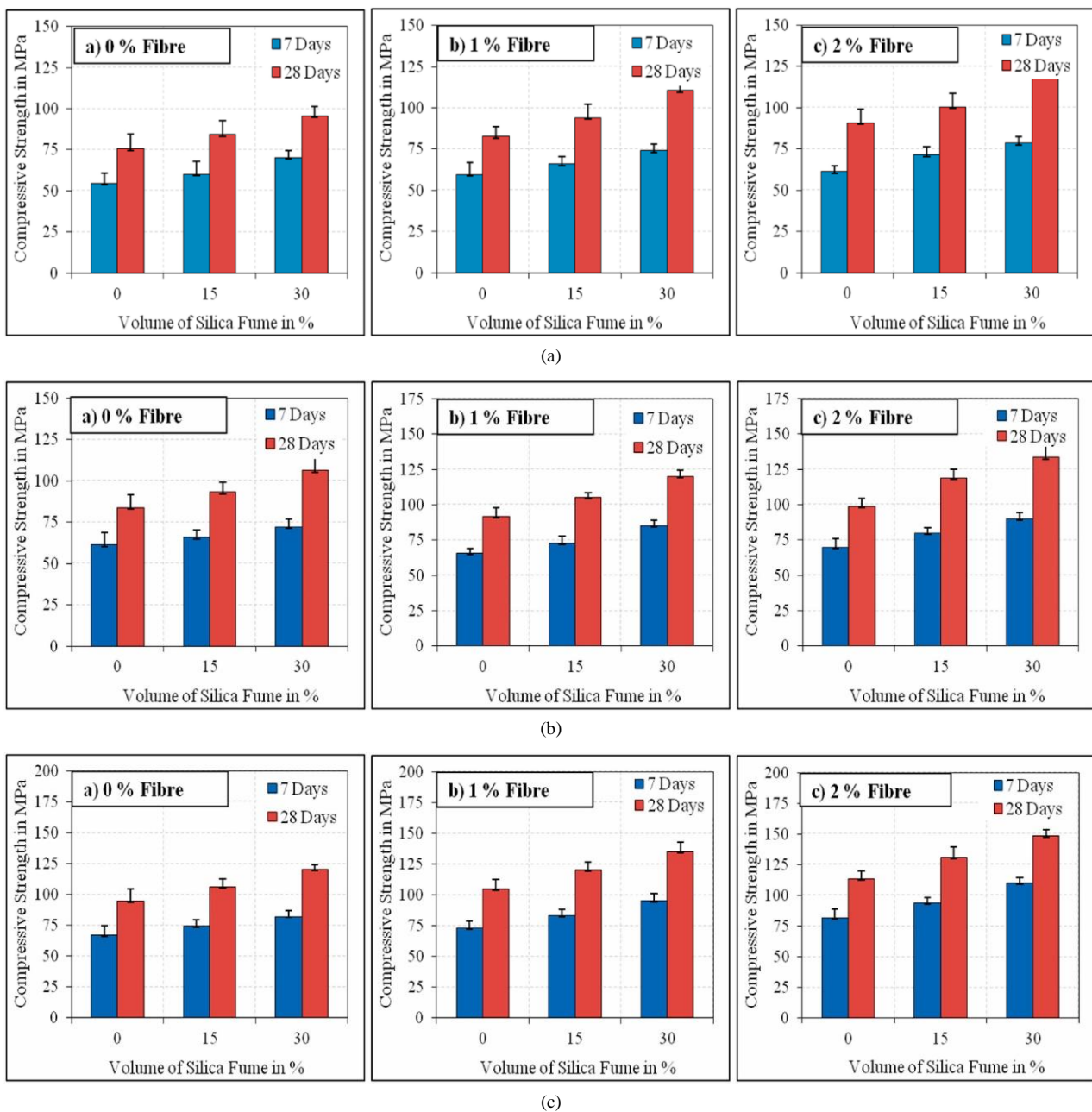
Figure 7. Compressive strengths of ultra high-performance geopolymer concrete specimens with (a) 20%, (b) 30%, and (c) 40% quartz content at 7- and 28-days curing [36]

2.3. Effect of Steel Fibers

Steel fibers provide reinforcement that strengthens UHP-GC. As a concrete reinforcer, steel fibers are identified as compact, distinct strands of steel with varying cross-sections. These strands possess an ideal aspect ratio ranging from approximately 20 to 100, showcasing their versatility. Moreover, these steel fibers are intentionally designed to be small, enabling their random dispersion throughout an unhardened concrete mixture using standard mixing procedures. Steel fibers reduce cracks in geopolymer concrete and enable it to exhibit ductile behavior. Liu et al. [30] developed UHP-GC using various sizes and ratios of steel fibers in the mix designs. The steel fibers for the geopolymer concrete are of varying lengths (6, 8, and 13 mm) and varying diameters (0.12 and 0.2 mm). The impact of steel fiber ratios on the compressive and flexural strength of geopolymer concrete is depicted in Figure 8. The compressive and flexural strength values of the concrete improved when the steel fiber content was increased. When the concrete specimens were designed with 3% steel fiber content, the highest compressive strength values were proven to be 170.3 and 157.7 MPa for steam and standard curing, respectively (Figure 8-a). The degree of improvement in the modulus of rupture of UHP-GC is dependent on the length of the steel fiber. In particular, the steel fiber direction and diffusion affect the flexural performance of UHP-GC in terms of the fibers' capability to bridge concrete microcracks [37-39]. Figure 8-b shows steel fibers' influence on the flexural strength of UHP-GC specimens. It is noticed that without steel fiber, the concrete's flexural strength with 1-day steam curing and 28-day standard curing were traced to be 8.7 and 4.6 MPa, respectively. When the concrete was added with steel fibers of 3%, its flexural strength values at steam and standard curing increased by 189.4 and 434.1%, respectively. The results also revealed that the compressive and flexural strength values of the concrete declined by increasing in the diameter of the fiber. It is also noticed that the concrete's compressive and flexural strength values increased by an increase in the length of fiber [30].

Aisheh et al. [31] clarified that steel fibers have profound impact on the mechanical properties of UHP-GC. The UHP-GC was prepared with mix ingredients of GGBS, micro silica, and steel fibers. The steel fibers used are characterized by 0.12 mm in diameter, 15 mm in length, 230 GPa elastic modulus, 2050 MPa tensile strength, and 7865 kg m^{-3} in density. The differing quantities of steel fibers used in the concrete are 1, 1.25, 1.5, 1.75, 2, and 2.25 % of total concrete volume. At 28-day curing, the highest compressive strength and ultimate flexural strength values of the concrete were traced to be 162 and 13.7 MPa, respectively. It was reported in the published work that harsh mixes in the fresh state of the concrete are the result of high steel fiber content of more than 1.75%. In another study, Aisheh et al. [40] reported the impact of steel fibers on the mechanical characteristics of UHP-GC. The UHP-GC was prepared by mixing GGBS, fly ash, and micro silica with various steel fiber contents of 0, 1, 2, and 3% by the total mass of binder. Using concrete specimens containing 0% steel fiber, the compressive strength and elastic modulus of UHP-GC were determined to be 102 MPa, and 27 GPa, respectively. When the concrete admixture was designed with 3% steel content, the concrete's compressive strength and elastic modulus were improved by 156 MPa and 32 GPa, respectively which reflected an increase in its compressive strength by 53% and modulus elasticity by 22%.

Similar patterns of compressive strength and modulus elasticity were achieved by previously published works using steel fibers in ultra-high-performance concrete (UHPC) [41] and steel fiber-reinforced geopolymer concrete [42]. Lao et al. [43] experimented the hardened properties of UHP-GC utilizing steel fibers. The UHP-GC was produced by mixing fly ash, GGBS, and silica fume in combination with different proportions of steel fibers, which are 2, 3, and 4% by the total volume of the binder. The steel fibers were tested, and their physical properties were discovered to be 0.2 mm diameter, 13 mm length, modulus elasticity of 210 MPa, and a density of 7.8 g cm^{-2}. The best experimental result indicated that the concrete's compressive strength was achieved at 199 MPa, with the addition of 2% steel fibers. In addition, an increase of steel fibers from 2 to 4% in the concrete resulted in its compressive strength increasing by 23 MPa, which is 222 MPa. The high elastic modulus of steel fibers contributed to the rise in compressive strength of the concrete.
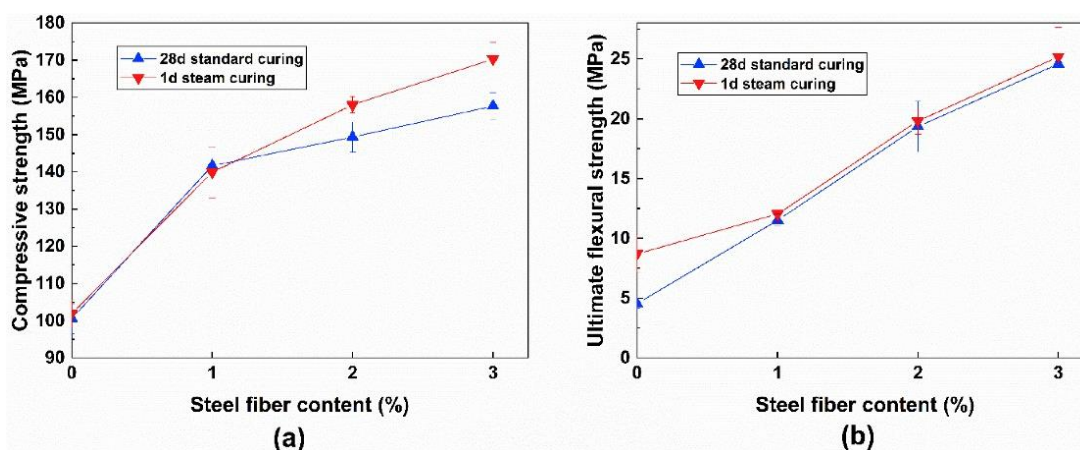
Figure 8. Influence of steel fiber content on (a) compressive and (b) ultimate flexural strengths of ultra high-performance geopolymer concrete [30]

Ambily et al. [16] evaluated the mechanical behavior of UHP-GC produced from GGBS, silica fume, and steel fibers. Out of the five UHP-GC mix designs, four are with steel fibers and one is without steel fiber. The steel fibers under the study have sizes of 0.16 mm in diameter and 13 and 6 mm in length. Without steel fiber, the highest compressive strength of the UHP-GC was noticed to be 124 MPa. The UHP-GC with steel fiber content of 1% (6 mm) and 2% (13 mm) was tested to have a maximum compressive strength of 175 MPa. The maximum flexural strength values for the concrete were evaluated to be 9.1 MPa, and 10.3 to 13.5 MPa for UHP-GC specimens without and with steel fibers, respectively. The strength improvement of the UHP-GC specimens was largely contributed by the capability of the steel fibers to decrease the concrete specimens' microcracks due to the fibers' reinforcing and strengthening effects.

The influence of steel fibers on UHP-GC's mechanical behavior was also reported by Liu et al. [15]. Apart from the steel fibers, GGBS, Class C fly ash, and silica fume were applied in the UHP-GC admixtures. The UHP-GC concrete specimens were varied with steel fiber dosages of 0, 1, 2, and 3% of the total binder. The size of each steel fiber is 0.12 mm in diameter and 13 mm in length. The effect of the steel fibers on compressive strength and elastic modulus of UHP-GC improved with various percentages of steel fibers is indicated in Figure 9. There was a progressive increase in both the compressive strength and elastic modulus of UHP-GC with increasing steel fiber content. Without steel fiber, the average compressive strength and elastic modulus of the UHP-GC specimens were measured as 101.4 MPa and 25.8 GPa, respectively. With 1% steel fiber content, both parametric values of the UHP-GC specimens elevated to 127.5 MPa and 29 GPa; respectively. At 3% steel fiber content, both parameters of UHP-GC specimens were noticed to be the highest at 154.9 MPa and 31.5 GPa, respectively, which are 52.9 and 22% respectively higher than the concrete specimens without steel fiber. The findings confirmed the significant impact of steel fibers at decreasing the microcracks of the concrete, thereby enabling the concrete specimens with steel fibers to better sustain loading impact compared to the ones without steel fiber.
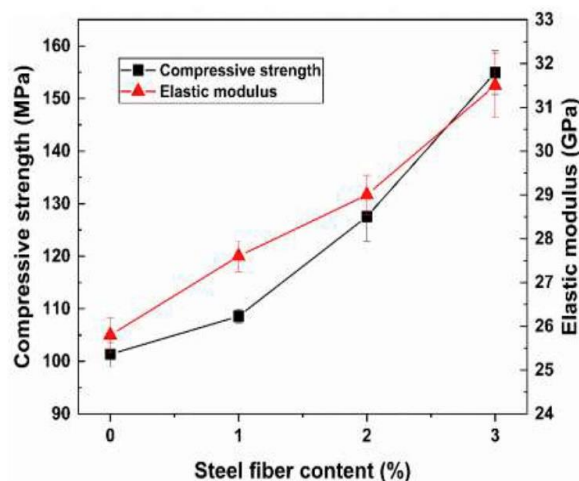
Figure 9. Compressive strength and elastic modulus of ultra high-performance geopolymer concrete specimens with various steel fiber content [15]

Mousavinejad & Sammak [44] examined the impact of steel fibers on the strength development of UHP-GC. GGBS and silica fume were incorporated into the UHP-GC. Each steel fiber was measured at 13 mm in length, 0.2 mm in diameter, with a density of 785 N m^{-3}, an elastic modulus of 200 GPa, and a tensile strength of 2000 MPa. Steel fibers were applied at various proportions (1, 1.5, and 2%) in the concrete's mix designs. In comparison with the control specimen, the test findings of UHP-GC specimens showed that raising the steel fiber content from 1 to 2% enhanced compressive strength from 137.96 to 150.61 MPa, and tensile strength from 6.48 to 7.73 MPa; respectively.

Liu et al. [45] assessed the effect of various types of steel fiber integration on the UHP-GC engineering characteristics. The UHP-GC was experimented utilizing GGBS, fly ash, and silica fume. In the investigation, three kinds of steel fibers were employed in total volume which are Long Steel Fiber (LSF), Short Steel Fiber (SSF), and Basalt Fiber (BF). Five UHP-GC specimens were readied, the first UHP-GC specimen (M1) was designed as the control one, the second one (M2) was generated with 2% LSF, the third one (M3) included 1% LSF and 1% BF, and the fourth one (M4) was incorporated with 2% SSF. The fifth one (M5) was produced with 2.5% LSF. The compression test results for the UHP-GC specimens showed that M1, M2, M3, M4, and M5 had compressive strength values of 94, 102, 110, 141, and 151 MPa, respectively. The test findings showed that inclusions of 2% SSF, 2.5% LSF, and 1%LSF and 1% BF improved the compressive strength of UHP-GC specimens when compared to 2% LSF. This shows that integrating steel fibers at an optimal dosage into UHP-GC yields a multitude of advantages, ranging from averting unexpected structural failures and enhancing fracture resistance, to mitigating crack widths, curbing shrinkage, and boosting both flexural and tensile strength, along with overall durability.

2.4. Effect of Polypropylene Fibers

Polypropylene fiber, also referred to as PPF, emerges as a remarkable synthetic fiber derived from the polymerization of propylene. This unique linear polymer offers a multitude of benefits, including its light weight, exceptional strength, impressive toughness, and significant resistance to corrosion. Mousavinejad & Sammak [46] found that polypropylene fibers (PPF) enhanced the strength characteristics of UHP-GC made of GGBS and silica fume. PPF are known to act as concrete reinforcer and minimize cracks in concrete. Under the study, the PPF content was fixed at 0.25% in the mix design of UHP-GC with varying steel fibers of 0.75, 1.25, and 1.75% by the total volume of the concrete. The fibers are characterized by a density of 910 kg m^{-3}, an elastic modulus of 3.5 GPa, and a tensile strength of 400 MPa. The length and diameter of the fiber were measured to be 6 mm and 0.035 mm, respectively. The compressive strength of the control UHP-GC specimen at 28-day was noted to be 112.65 MPa. However, an addition of 1.75% steel fibers into the UHP-GC resulted in an improved compressive strength of 145.31 MPa, and this implies a 29% strength enhancement as compared with the control one. With the addition of 0.25% PPF and 1.75% steel fibers to the UHP-GC, the compressive strength marginally increased to 146.12 MPa, which demonstrates a 29.7% strength enhancement when compared to the control one. The main reason for such a significant strength improvement in the fiber treated UHP-GC is the ability of the PPF to create a more cohesive bonding in the concrete, thereby reducing the deformation and formation of cracks after failure.

Aisheh et al. [40] studied the impact of PPF on the engineering behavior of UHP-GC characterized by GGBS and micro silica. The PPF were noted to have a density of 915 kg m^{-3}, a tensile strength of 430 MPa, and an elastic modulus of 3.65 GPa. The length and the diameter of the PPF under study were 8 mm and 0.033 mm, respectively. Two mix designs which are based on 0 and 0.25% PPF from the total volume of the binder in the UHP-GC were experimented. The result revealed that there was a considerable enhancement in the engineering properties of UHP-GC improved with PPF. A moderate increase was noted in the compressive strength of the PPF improved UHP-GC when compared to the control one. The finding further strengthened the positive evidence of PPF at reinforcing the UHP-GC, thereby decreasing its plastic and drying shrinkage.

The PPF's effect on the strength properties of UHP-GC was also discovered by Tayeh et al. [32]. GGBS, fly ash, and micro silica were applied as the ingredients in the geopolymerization of UHP-GC. In the UHP-GC specimens, the fibers varied at 0, 0.75, 1.75, and 2.75% by the total volume of concrete. The PPF was examined to have a failure strain of 3.5%, a tensile strength of 275 GPa, an elastic modulus of 2.95 GPa, and a specific weight is 940 kg m^{-3}. The PPF's length and diameter are 50 mm and 0.032 mm, respectively. The compressive strength and elastic modulus findings of the UHP-GC specimens are illustrated in Figure 6. It was noticed that PPF addition in UHP-GC improved its compressive strength and elastic modulus. When 35% of micro silica was used, the inclusion of 0, 0.75, 1.75, and 2.75% PPF increased the concrete's compressive strength by 20, 19, 15, and 17% respectively, compared to the concrete specimens without micro silica. While, when the micro silica content is 25%, the inclusion of 0, 0.75, 1.75, and 2.75% PPF increased the elastic modulus by 8.3, 2.5, 2.4, and 2.3%, respectively in comparison to samples without silica fume. The reason for the notable improvement in the compression behavior of the PPF improved UHP-GC is the fibers could function as a bridging agent that strengthened the concrete by minimizing the concrete's crack formation at failure.

2.5. Effect of Waste Glass and Ceramic

Waste glass was explored by Tahwia et al. [33] as a strength enhancing ingredient of UHP-GC. Other than waste glass powder, GGBS and silica fume were incorporated into the UHP-GC. Several waste glass contents (0, 7.5, 15, and 22.5%) were applied as partial substitutes of sand in the concrete. The waste glass has a specific gravity of 2.49, a fineness modulus of 2.4, and a water absorption of 0.12%. The experimental findings revealed that raising the quantity of waste glass to the optimal level in the concrete's mix design resulted in an increase of its compressive strength. However, inclusion of 22.5% waste glass in the concrete reduced its compressive strength from 126 to 121 MPa in comparison to the control one. The decrease in the strength was linkable to the glass's smooth surface, which resulted in insufficient bonding between the glass aggregate and the components of the geopolymer in the concrete. It was apparent that the internal gaps caused by the angularity of glass particles had a detrimental effect on the concrete's compressive strength.

Tahwia et al. [47] further analyzed the strength properties of UHP-GC improved with crushed glass. Other than the crushed glass, GGBS and silica fume were included in the admixtures of the UHP-GC. The crushed glass was varied in the mix designs at 7.5, 15, and 22.5% by as partial volume substitute of sand in concrete. The results of compression tests on the UHP-GC specimens with crushed glass are shown in Figure 10. When crushed glass was set at 7.5% in the mix design, the highest strength at 28- day was traced to be 149 MPa which is slightly lower than the control one at 152 MPa. The results also proved that when the crushed glass replacement and curing age of the concrete increased, the corresponding compressive strength also increased. The maximum compressive strength of 159 MPa was reached by utilizing 22.5% crushed glass in the concrete under 56-day curing. The UHP-GC demonstrated enhanced compression efficiency due to the crushed glass inclusion, leading to the substantial development of calcium aluminate silicate hydrate (C-A-S-H) products. This progress arises from the amalgamation of geopolymer composites with reactive silicon dioxide-containing glass, generating favorable outcomes in terms of compression performance.
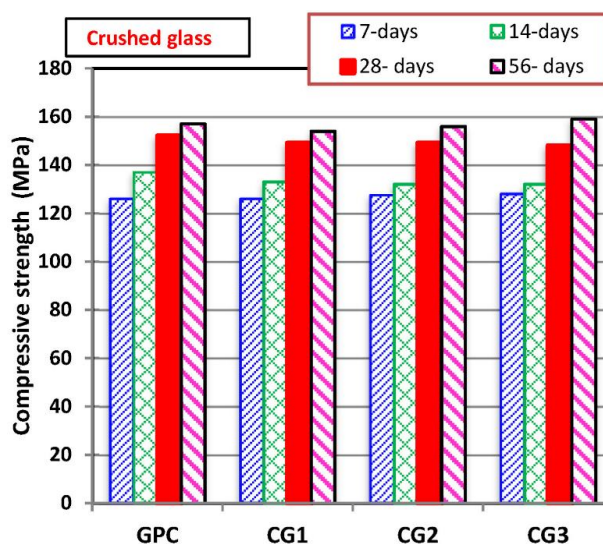
Figure 10. Impact of crushed glass on the compressive strength of ultra high-performance geopolymer concrete [47]

In an improved research work, Tahwia et al. [48] assessed the impact of waste glass and waste ceramic on the compressive strength of UHP-GC. GGBS and silica fume functioned as the precursor of the concrete. Various amounts of waste glass and waste ceramic were used as a partial replacement of sand in the concrete, with the partial sand replacement ranged from 7.5 to 22.5% by concrete volume. The UHP-GC specimens were exposed to different heat temperatures ranging from 27 to 800°C for a duration of 1.5 hours with a goal to gage their heat resistance. After 56-day ambient temperature curing, the control concrete specimens exhibited the highest compressive strength at 137 MPa.

A slight decrease in the concrete's compressive strength was observed when incorporating 22.5% waste glass, resulting in a strength of 135 MPa. Conversely, the incorporation of 22.5% waste ceramic in the concrete led to a 14% decrease in compressive strength, reaching 119 MPa compared to the control one. At 200°C, the control specimen achieved a compressive strength of 164 MPa, while the UHP-GC specimen with 22.5% waste glass was tested to have 157 MPa compressive strength. However, the concrete specimen with 22.5% waste ceramic experienced a decrease in compressive strength, reaching 124 MPa after the heat exposure. At 800°C, the concrete specimen with 22.5% waste glass exhibited the highest residual strength of 41 MPa. It is necessary to highlight that the concrete specimen with 22.5% waste ceramic achieved a residual strength of 22 MPa. The enhancement in concrete's compressive strength resulting from the inclusion of waste glass could be attributed to the cohesive interaction between waste glass and geopolymer gels. Moreover, the strengthening of the geopolymerization process in the UHP-GC specimens with waste glass due to heat curing is the reason for the increase in strength beyond 200°C.

Liu et al. [49] evaluated the impact of using ceramic balls as coarse aggregate on the UHP-GC mechanical characteristics. GGBFS, fly ash, and silica fume were used in the formulation of UHP-GC mix designs. The ceramic balls possess chemical characteristics including an alumina (Al_2O_3) content ranging from 47 to 56%, and silica (SiO_2) content exceeding 93%, a density of 1800 kg m^{-3}, water absorption below 2%, abrasion less than 5%, and a hardness of 7-8 on the Mohs scale. Each ceramic ball had a diameter of 10 mm. Three types of UHP-GC specimens were tested in the study: the first served as a control concrete specimen, the second incorporated 25% ceramic balls by total volume of concrete, and the third incorporated 20% ceramic balls and 1.5% steel fibers by total volume of concrete. Steam curing at 900°C for 48 hours was applied in this investigation, with the concrete specimens covered by a plastic sheet. The compressive strength and elastic modulus values of the UHP-GC specimens are as follows: 94 MPa and 38.9 GPa for the control concrete specimen, 97 MPa and 40.1 GPa for the concrete specimen with 25% ceramic balls, and 114 MPa and 49.9 GPa for the concrete specimen with 20% ceramic balls and 1.5% steel fibers, respectively. The best strength results from the study are based on an optimal combination of ceramic balls and steel fibers in the concrete. The presence of high-strength coarse aggregate can be ascribed to the increment in the UHP-GC's strength achieved through the utilization of ceramic balls.

3. Influence of Alkaline Activation and Sodium Hydroxide Molarity on the Strength Development of Ultra High-Performance Geopolymer Concrete

The bonding and strength gain of UHP-GC are influenced by alkaline activation and molarity. A study by Aisheh et al. [40] revealed that the mechanical characteristics of UHP-GC were obviously affected by the ratio of sodium silicate to sodium hydroxide (SS/SH) and the molarity of sodium hydroxide (SH). UHP-GC specimens with various alkaline activator solutions, GGBS, and micro silica were tested following various SS/SH ratios and SH molarities. The results demonstrated that increasing the SS/SH ratio caused a decline in the water/solid binder ratio (w/b) and subsequently

improved the compressive strength of UHP-GC (Figure 11). Specifically, when the SS/SH ratio increased from 1.5 to 3.5, the w/b ratio decreased by 7 and 9%, resulting in a corresponding increase in concrete compressive strength of 7 and 14% compared to an SS/SH ratio of 1. Likewise, an increase in SH molarity yielded a decline in the w/b ratio and a concurrent elevation in the compressive strength of the concrete. In instances where the SH molarity was heightened from 6 to 14 within the UHP-GC specimens, the w/b ratio registered reductions of 18, 14, and 10% for corresponding SS/SH ratios of 1.5, 2.5, and 3.5. Correspondingly, for identical SS/SH ratios, the concrete's compressive strength saw increments of 38, 33, and 31%. Intriguingly, the combined augmentation of both SH molarity and SS/SH ratio culminated in a striking 46% surge in the compressive strength of the UHP-GC specimens. These discoveries underscore the critical nature of optimizing the ratios of SS/SH and SH molarity during the production of robust UHP-GC. The ramifications of this published research hold particular significance within the construction realm, where the demand for high-strength concrete remains steadfast. By harnessing the potency of the optimum SS/SH and SH molarity ratios, it becomes conceivable to curtail the w/b ratio, subsequently enhancing the durability of concrete structures. Overall, the outcomes of this study yield valuable insights into the domains of material science and mechanical attributes intrinsic to UHP-GC, thereby providing strategic leverage for elevating the performance benchmarks of concrete across diverse applications.
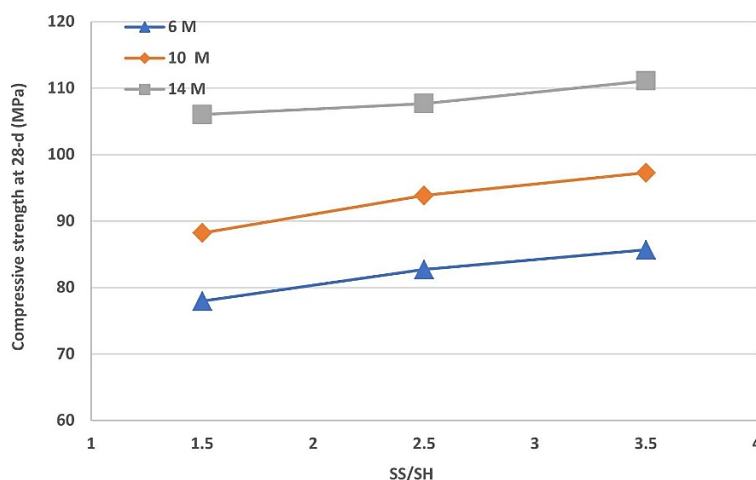
Figure 11. Correlations between the 28-day compressive strength and the sodium silicate to sodium hydroxide ratio and sodium hydroxide molarity of ultra high-performance fiber reinforced geopolymer concrete [40]

Mousavinejad & Sammak [46] evaluated the influence of SS/SH ratio and SH molarity on the properties of UHP-GC, with GGBS and silica fume as the precursors. The alkaline activator solution consisted of 98% pure sodium hydroxide flakes and sodium silicate with a solid content of 44.5% and a modulus ratio of 2.07 (55.5% solution). Concrete mix designs were prepared with SS/SH ratios of 1, 2, and 3; and SH molarity of 8, 12, and 16 and the 28-day compressive strength results of UHP-GC specimens are depicted in Figure 12. The results of the compression tests after 28 days of curing showed that increasing the SS/SH ratio from 1 to 3, with an SH molarity of 8, increased the concrete compressive strength from 105.13 to 116.34 MPa. Similarly, when the SS/SH ratio was 3, increasing the SH molarity from 8 to 16 increased the concrete's compressive strength from 116.34 to 130.11 MPa.
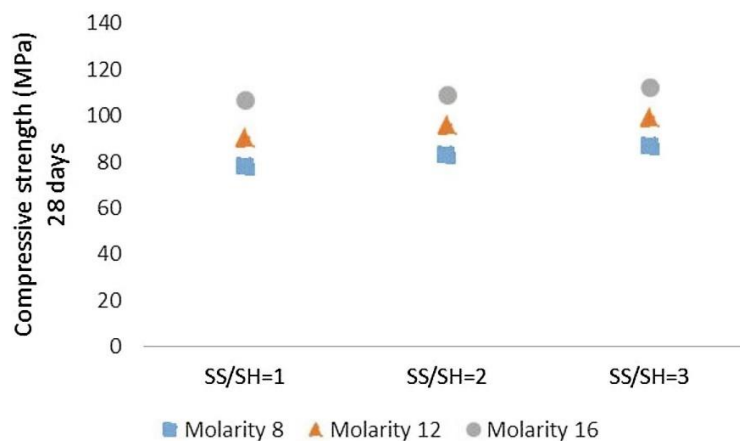
Figure 12. The 28-day compressive strength development of ultra high-performance geopolymer concrete with ground granulated blast furnace slag and silica fume as the precursors at various sodium silicate to sodium hydroxide ratios and sodium hydroxide molarities [46].

In another experimental research, the effects of SS/SH ratios and SH molarity on the compressive strength of UHP-GC specimens containing GGBS and silica fume were further analyzed by Mousavinejad & Sammak [50]. The UHP-GC specimens were produced with SS/SH ratios of 1, 2, and 3, and SH molarity of 8, 12, and 16. The mix proportions of the UHP-GC specimens are listed in Table 1. The experimental results showed that increasing the SH molarity from 8 to 16 M reduced the water to solid binder ratio from 16.41 to 8.64%, resulting in a 36.47 and 31.31% increase in the concrete's compressive strength, respectively (Table 2). The increase in the concrete's compressive strength with higher SH molarity is attributed to increased aluminosilicate dissolution and polymer chain formation [51]. Other than that, increasing the SS/SH ratios from 1 to 3 resulted in a 6.44% and 11.44% increase in UHP-GC's compressive strength, respectively. Based on the published work, it can be summarized that the improvement in UHP-GC's compressive strength is directly related to the SS/SH ratio and SH molarity. Based on the data presented in Table 2, the split tensile strength and elastic modulus of the UHP-GC specimens also showed similar trends of development with the SS/SH ratio and SH molarity.

Table 1. Mix proportions of ultra high-performance geopolymer concrete specimens containing ground granulated blast furnace slag and silica fume [50]

Mixture	GGBS (kg m^{-3})	Silica fume (kg m^{-3})	Sodium hydroxide solution (kg m^{-3})	Sodium silicate solution (kg m^{-3})	Quartz sand (kg m^{-3})	SS/SH ratio	NaOH Conc. (Molarity)	Water to binder ratio (w/b)
SS/SH1M8	850.23	283.4	170.04	170.04	930.4	1	8	0.175
SS/SH2M8	850.23	283.4	113.36	226.72	940.9	2	8	0.165
SS/SH3M8	850.23	283.4	85.02	255.06	945.9	3	8	0.160
SS/SH3M12	850.23	283.4	85.02	255.06	945.9	3	12	0.153
SS/SH3M16	850.23	283.4	85.02	255.06	945.9	3	16	0.146

Table 2. Mechanical properties of ultra high-performance geopolymer concrete specimens containing ground granulated blast furnace slag and silica fume (Note: f_c = Compressive strength, f_t = Split tensile strength, E_c = Elastic modulus) [50]

Mixture	Age of testing (day)	f_c (MPa)	f_t (MPa)	E_c (GPa)
Series 1				
SS/SH1M8	28	105.13	5.06	41.78
SS/SH2M8	28	111.25	5.12	42.64
SS/SH3M8	28	116.34	5.26	43.72
Series 2				
SS/SH3M8	28	116.34	5.26	43.72
SS/SH3M12	28	122.21	5.62	44.61
SS/SH3M16	28	130.11	6.14	45.2
Series 3				
SS/SH3M16	3	113.14	5.19	43.12
SS/SH3M16	7	118.31	5.31	44.03
SS/SH3M16	28	130.11	6.14	45.2

Wang et al. [35] explored the impact of SH molarity on the mechanical properties of UHP-GC specimens using low-calcium fly ash, calcium aluminate cement (CAC), and varying dosages of silica fume from 5 to 30%. Different SH molarities of 10 M, 12 M, and 14 M were used in the UHP-GC specimens to study the effect of SH concentration on their compressive strength. The results showed that increasing the SH molarity to 14 M increased the concrete's compressive strength to 91 MPa, which was 9.6% and 6.3% higher than the concrete specimens with SH molarities of 10 M and 12 M, respectively. The increase in the concrete's compressive strength can be attributed to the higher SH concentration, which promotes geopolymerization by dissolving the solid raw materials [52, 53].

Lao et al. [54] analyzed the impact of sodium carbonate (Na_2CO_3) on the engineering behavior of UHP-GC specimens. The study focused on using fly ash, GGBS, and silica fume to produce UHP-GC specimens with an alkaline activator comprised of Na_2CO_3 and sodium silicate (Na_2SiO_3). Three UHP-GC specimens with different alkaline activator percentages were tested: 100% Na_2CO_3 and 0% Na_2SiO_3, 50% Na_2CO_3 and 50% Na_2SiO_3, and 0% Na_2CO_3 and 100% Na_2SiO_3. The compression test results indicated that 100% Na_2CO_3 UHP-GC had a compressive strength of 135.8 MPa, 50% Na_2CO_3 and 50% Na_2SiO_3 UHP-GC had a compressive strength of 186 MPa, and 100% Na_2SiO_3 UHP-GC had a compressive strength of 179 MPa. Based on these findings, the optimal alkaline activation for the UHP-GC specimens was determined to be 50% Na_2CO_3 and 50% Na_2SiO_3. A similar trend of the results was also observed in the tensile strength development of the UHP-GC specimens.

4. Microstructure and Chemical Investigations of UHP-GC

After reviewing the photomicrographs of Ultra High-Performance Geopolymer Concrete (UHP-GC) samples, Bahmani & Mostofinejad [55] clarified that black marks in a UHP-GC microstructure indicated the presence of micro silica which participated reactively with an alkaline activator to generate calcium aluminosilicate hydrate (C-A-S-H) gels that eventually contributed to cementation in the geopolymeric network. The C-A-S-H gels are amorphous and semi-crystalline in nature and their formation in UHP-GC is promoted when GGBS is partially replaced with a pozzolanic additive such as metakaolin. Figure 13 compares the microstructures of UHP-GC between the sample with 750 kg m^{-3} GGBS: 235 kg m^{-3} silica fume and the one with 750 kg m^{-3} metakaolin: 235 kg m^{-3} silica fume with reference to the study of Alharbi et al. [56]. It should be noted that other than the precursor, each UHP-GC sample also consists of 885 kg m^{-3} quartz sand, 220 kg m^{-3} quartz powder, 85.7 kg m^{-3} sodium hydroxide solution, 214.3 kg m^{-3} sodium silicate, 150 kg m^{-3} water, and 45 kg m^{-3} superplasticizer. The microstructure of the UHP-GC sample with GGBS and silica fume (Figure 13-a) has a higher degree of compactness with semi-crystalline morphology compared to the one with metakaolin and silica fume (Figure 13-b). It is seen in Figure 13-b that the combination of metakaolin and silica fume as the precursor for the concrete geopolymerization resulted in an amorphous microstructure with no distinctive nanocrystalline growth observable. The microstructure evidence reflected that the UHP-GC sample with GGBS and silica fume has denser and more robust geopolymeric bonding structures compared to the one with metakaolin and silica fume. The energy dispersive x-ray (EDX) outcomes corresponding to the UHP-GC samples shown in Figures 13-a and 13-b are illustrated in Figures 14-a and 14-b, respectively. The EDX test on the UHP-GC sample with GGBS and silica fume resulted in the development of C-A-S-H gels, which are reflected by the high peaks of Ca, Al, Si, and O elements as evident in the EDX result of Figure 14a. In another EDX test, the result showed that the UHP-GC sample with metakaolin and silica fume is characterized by high peaks of Na, Ca, Al, Si, and O elements which indicated the presence of sodium aluminosilicate hydrate (N-A-S-H) and C-A-S-H gels in its cementation matrix (Figure 14-b). When optimized with silica fume, GGBS played a better role at minimizing the voids in UHP-GC in comparison to metakaolin due to its greater capability to yield more geopolymer products which were caused by its intensified polycondensation reaction.

(a)   (b)
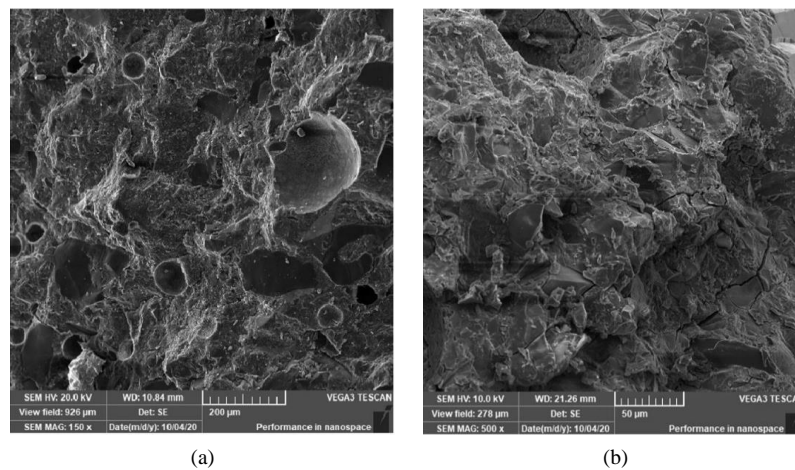
Figure 13. Scanning electron micrographs of ultra-high performance geopolymer concrete sample improved with (a) ground granulated blast furnace slag and silica fume and (b) metakaolin and silica fume [56]

(a)

(b)
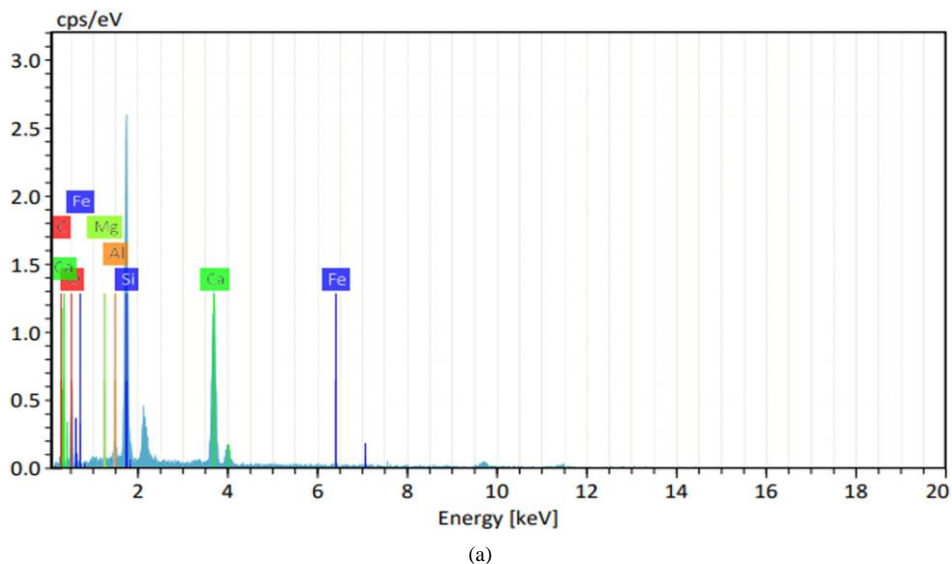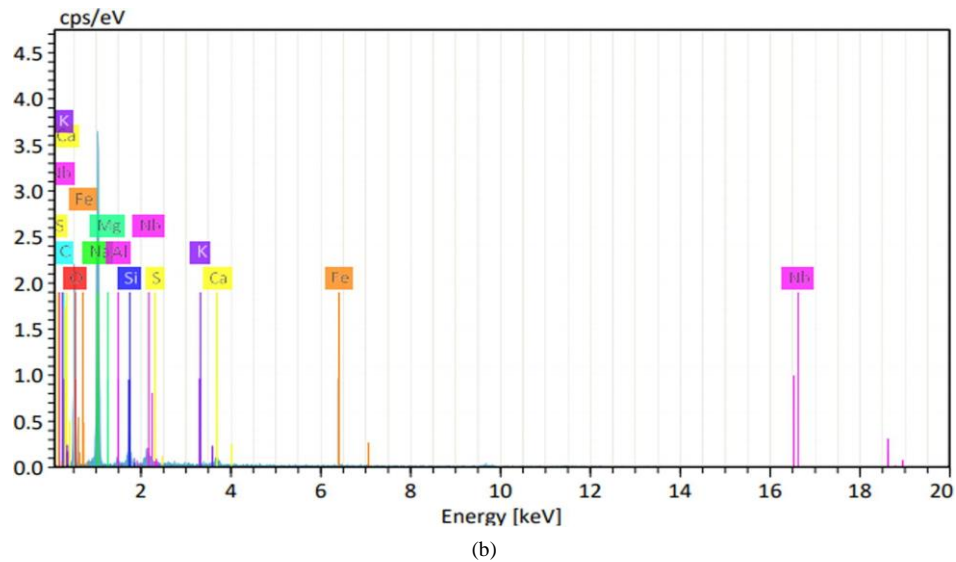
Figure 14. Energy dispersive x-ray result of ultra-high performance geopolymer concrete sample improved with (a) ground granulated blast furnace slag and silica fume and (b) metakaolin and silica fume [56]

Similar microstructures of UHP-GC samples can be traced from the published paper of Aisheh et al. [31]. Aisheh et al. [31] assessed the implication of adding steel fibers and silica fume on the mechanical performance of UHP-GC specimens. It should be noted that a maximum compressive strength of 156 MPa and a high elastic modulus of 32 GPa were tested for the UHP-GC specimen optimized with 3% steel fibers [31]. The respective parametric values of the UHP-GC specimen were found to be 53 and 22% higher than the specimen without steel fiber. Figure 15 demonstrates that the scanning electron micrographs of two UHP-GC samples are characterized by dense micropatterns. The dissolution of aluminates and silicates in the process of the concrete's geopolymerization is evident in Figure 15-a. The geopolymer binders in the forms of N-A-S-H and N-(C)-A-S-H gels are identified in Figure 15-b. The results confirmed that the UHP-GC samples underwent a polycondensation process, leading to the formation of a three-dimensional tecto-aluminosilicate framework, which is indicative of geopolymer formation. Geopolymerization effectively obstructs the interconnection of tiny pores by forming a more compact geopolymer gel matrix [57]. Dense microstructures of UHP-GC samples were also observed in the scanning electron micrographs from the studies of Aydin & Baradan [58] and Mehta & Siddique [59].
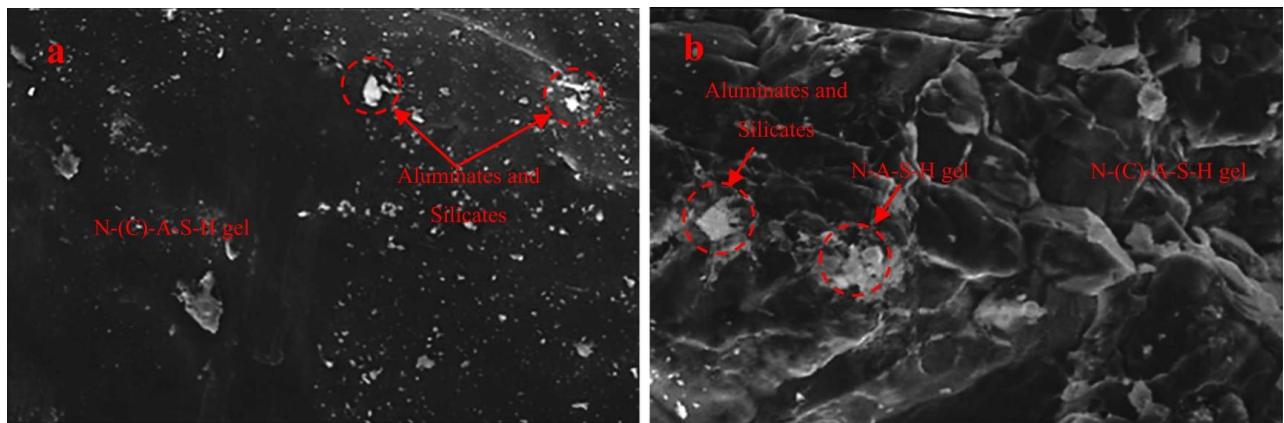
Figure 15. Scanning electron micrograph of the ultra-high-performance concrete sample indicating (a) the dissolved aluminates and silicates from the process of geopolymerization and (b) formation of N-A-S-H and N-(C)-A-S-H gels due to geopolymerization [31].

Tahwia et al. [48] explored the impact of temperatures ranging from 27 to 800°C, on the photomicrographs of UHP-GC samples with 22.5% waste glass (WG) or waste ceramic (WC) as the partial sand replacement. Figure 16 compares the microstructures of the UHP-GC samples with and without WG or WC between the lowest and the highest temperatures. It is shown in the figure that the pores of all UHP-GC samples were enlarged after exposure to 800°C. In particular, the UHP-GC sample with WG has the least pore development when compared with the other two samples after heating at the elevated temperature. The discovery is supported by the fact that at 800°C, the residual strength of the UHP-GC specimens with WG were found to vary from 27 to 32% and the range is higher than that of the ones with

WC (18 to 24%). The microstructure proofs can be associated with the x-ray diffraction peaks of the UHP-GC samples which were heated at temperatures varying from 27 to 800°C as shown in Figure 17.

All the UHP-GC samples demonstrated high peaks of minerals such as calcite, quartz, akermanite, mullite, gehlenite, albite, microcline, nepheline, and alite. At 800°C, the emergence of akermanite is discerned, a connection previously unattributed to the porous structure of UHP-GC. Remarkably, within the GP22.5WG sample, extra peaks emerged, which are linked to hydrogarnet, stemming from the slower deterioration of the geopolymer gel network and calcite even post exposure to 800°C (Figure 17-b). There was notable presence of akermanite and sorosilicate phases in the UHP-GC samples exposed to the high temperature. These crystalline formations potentially induced a shift in pore structure, spanning from microscopic to mesoscopic, potentially reaching macroscopic dimensions. Conversely, the vanishing of C-(N)-A-S-H became evident following exposure to 800°C in the GP22.5WC sample (Figure 17-c). These discoveries proved that the UHP-GC sample with WG has better heat resistance compared to that with WC.
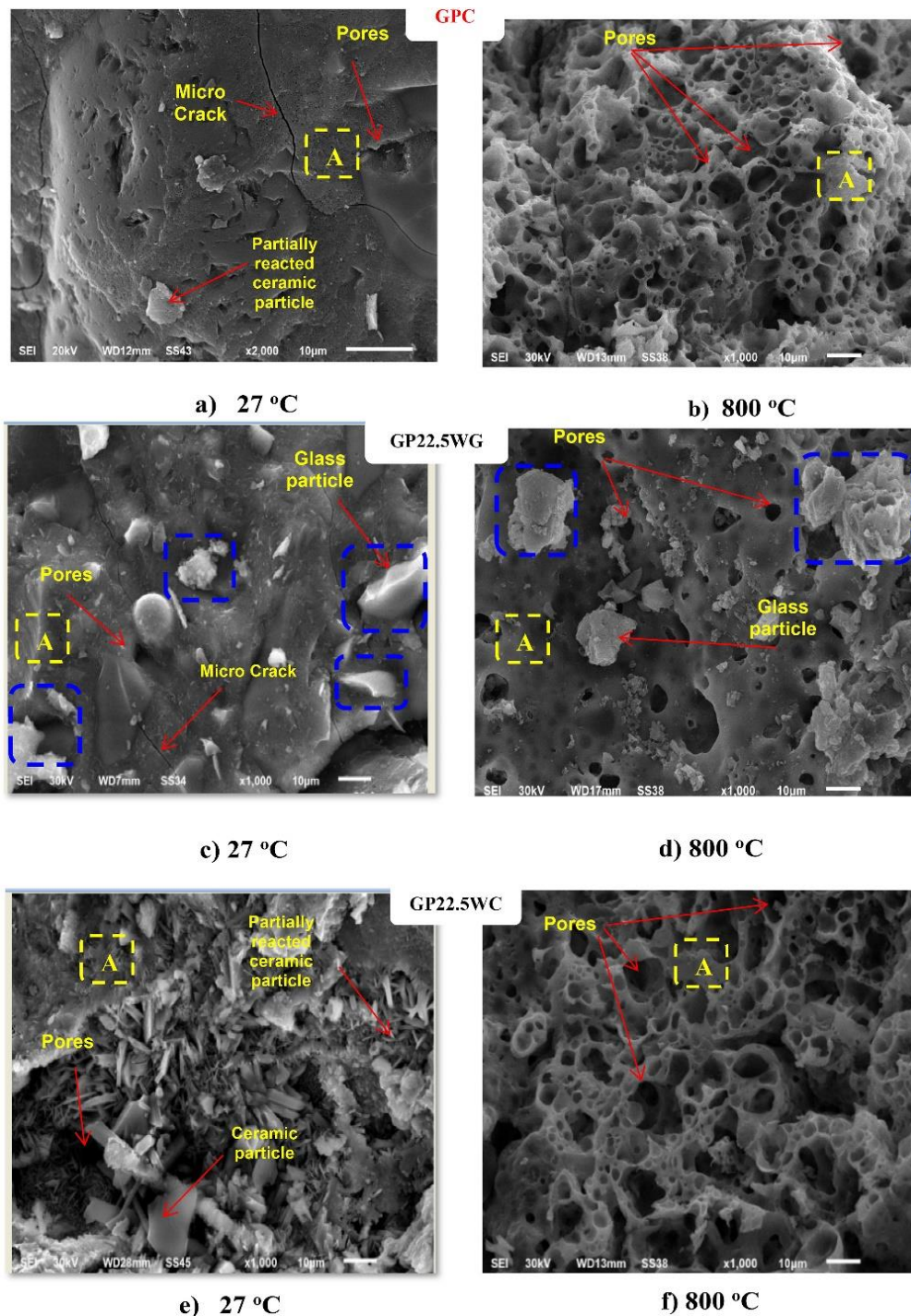
Figure 16. Scanning electron microscopic images of ultra high-performance geopolymer concrete samples after exposure to 27 and 800°C [48]
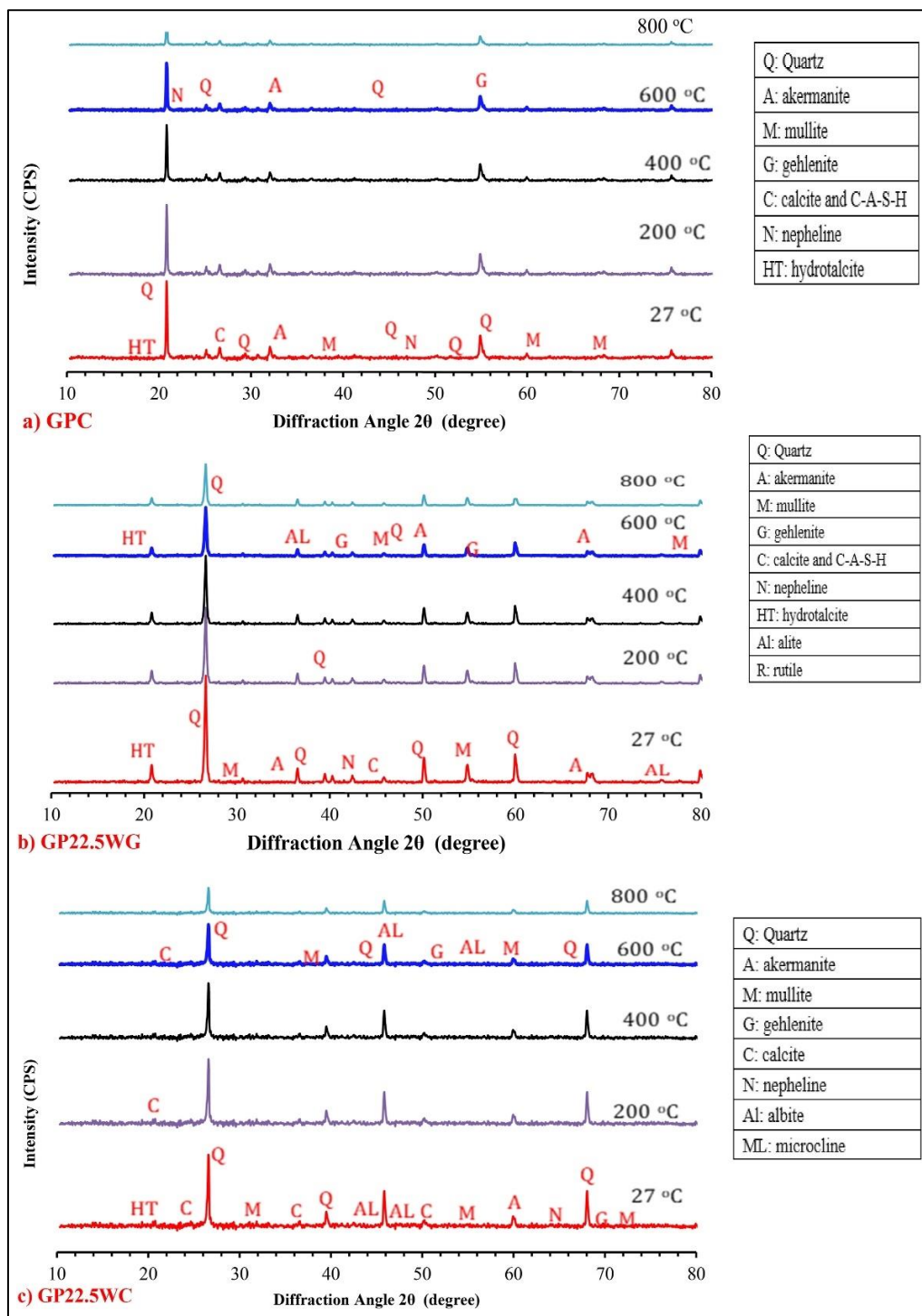
Figure 17. X-ray diffraction patterns of ultra high-performance geopolymer concrete samples at different temperatures [48]

The microstructures and chemical properties of UHP-GC were also investigated by Wang et al. [35]. Wang et al. [35] produced UHP-GC by activating a mixture of calcium aluminate cement (CAC), Class F fly ash, and silica fume with an alkali mixture which comprised of sodium hydroxide and sodium silicate solution. Figure 18 reveals the effect of silica fume on the microscopic images of the UHP-GC samples with 10% CAC. The microstructure exhibited a pervasive dispersion of fly ash particles, presenting a distinctly spherical form. This characteristic, absent in silica fume-free UHP-GC sample (SF-10-0), stood out prominently. Notably evident were the observable presence of cracks and voids in the UHP-GC sample without silica fume. For the UHP-GC sample with 10% silica fume (SF-10-10), notable alterations in morphology are observed, characterized by a compact microstructure and a diminished presence of unreacted particles. These changes elucidate the higher compressive strength exhibited by the SF-10-10 UHP-GC samples in comparison to the UHP-GC samples lacking silica fume in the investigation. The compact microstructure observed in the UHP-GC sample is comparable to that of OPC concrete from the study of Wong et al. [60]. Both samples

exhibited a dense cement matrix with limited void spaces. Upon increasing the dosage of silica fume to 20%, the UHP-GC sample designated as SF-10-20 exhibited discernible agglomeration of silica fume particles. This discovery aligns with the study's conclusion that the compressive strength of SF-10-20 specimen is inferior to SF-10-10 specimen due to the presence of internal flaws.
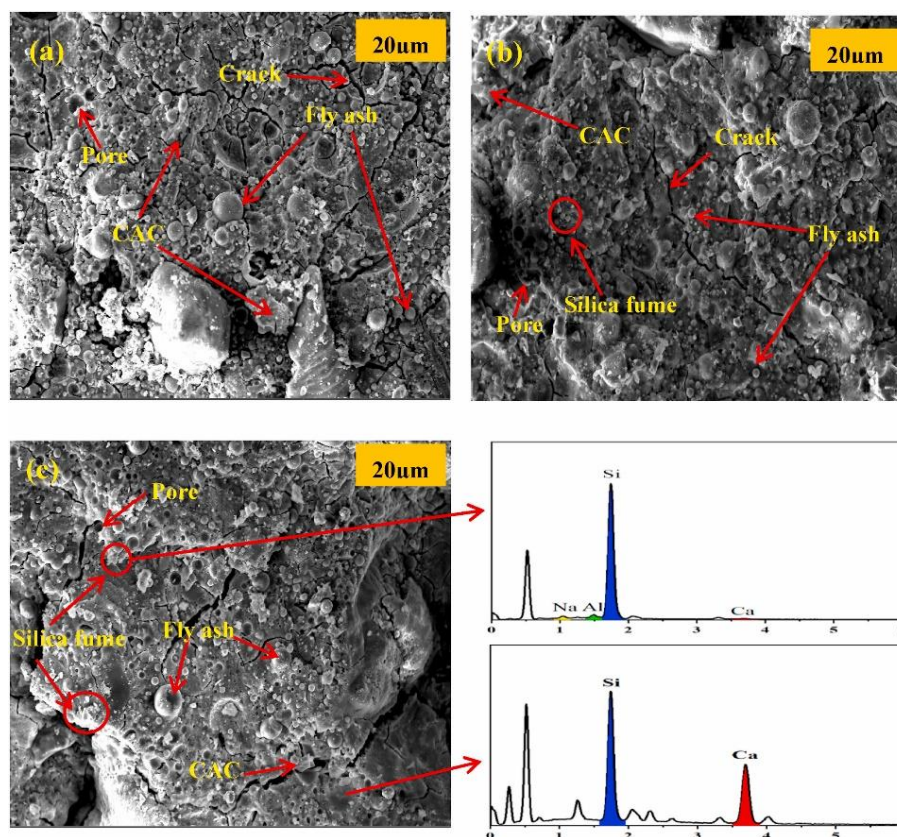
Figure 18. Effect of silica fume on the microstructures and energy dispersive x-ray of ultra high-performance geopolymer concrete samples with 10% calcium aluminate silicate: (a) SF-10-0, (b) SF-10-10, (c) SF-10-20 [35]

The corresponding XRD results of the UHP-GC samples of Figure 18 are depicted in Figure 19. Irrespective of the silica fume dosage, a distinct spectral feature was observed in all three UHP-GC samples at an angle of approximately 2θ, ranging from 20° to 40°. This spectral halo indicates the presence of sodium aluminosilicate gel (N-A-S-H), which is widely recognized for its influential role in the enhancement of strength in geopolymeric materials. Distinct diffraction peaks were identified at 26.5° and 35.5° of 2θ, proving the existence of unreacted fly ash and CAC after the polycondensation reaction. Besides, the diffraction peaks appearing at 2θ = 29.4° were attributed to the development of C–S–H gels. Previous research has also reported the emergence of C–S–H gels in an alkali-activated fly ash system [61] or a CAC system [62], due to the inclusion of silica fume. Apart from the simultaneous presence of N-A-S-H gels and C–S–H gels, the existence of gismondine and calcium aluminium silicate hydrate (also identified as Linde A) was also detected, albeit in limited quantities. Furthermore, the inclusion of silica fume in the UHP-GC sample resulted in a reduction in the intensity of the peak associated with quartz, suggesting a higher dissolution of silica during the process of alkaline activation [63].

An observation arises from the SF-10-10 specimen, as it not only exhibited the highest compressive strength, but its sample displayed the lowest intensity quartz peak based on the outcomes of the x-ray diffraction test. The interstitial spaces between solid grains hosted a uniform dispersion of unreacted silica fume particles, a phenomenon that ushered in a compact microstructure, subsequently enhancing the overall robustness of the UHP-GC specimen. The minerals that were not fully reacted can serve as fillers to enhance the strength of the geopolymer concrete, thereby significantly contributing to its overall durability [64]. Consequently, the compressive strength of the SF-10-10 specimen is greater than SF-10-0 specimen. Higher value of silica fume dosage is directly linked to an increased presence of unreacted silica fume content in the UHP-GC sample. This abundance of unreacted silica fume particles congregated and amalgamated, giving rise to structural imperfections that in turn led to a decrement in the strength of the UHP-GC specimen. This substantiates the finding that the compressive strength of the SF-10-20 specimen inherently falls short in comparison to that exhibited by the SF-10-10 specimen.
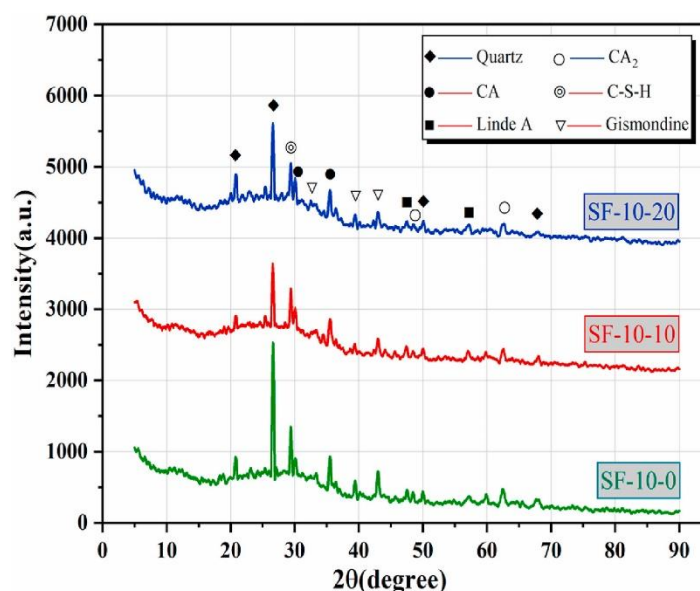
Figure 19. Effect of silica fume on the x-ray diffraction patterns of ultra high-performance geopolymer concrete samples with 10% calcium aluminate cement (CAC) [35]

5. Conclusions

The following points are concluded after a coherent review of published works related to this article.

- The most effective combination of GGBS and fly ash (with a fly ash to GGBS ratio of 0.25), used as a binary precursor, demonstrated a remarkable influence on the strength attainment of UHP-GC specimens when maintained at an optimal water-to-precursor ratio of 0.22. This phenomenon was caused by the presence of calcium oxide (CaO), which elevated the alkalinity of the geopolymer mixture, consequently augmenting the dissolution process of silica and alumina components essential for the formation of UHP-GC specimens. This, in turn, fostered the generation of aluminosilicate oligomers, crucial for solidifying UHP-GC. The introduction of 3% steel fiber content not only contributed to the mitigation of microcracks but also enhanced UHP-GC's capacity to reduce them. Beyond microcrack suppression, steel fibers played a role in fortifying the UHP-GC surface, lowering its permeability, and thereby optimizing surface durability, bolstering strength progression, and elevating impact resistance.

- The analysis revealed that setting the SS/SH ratio at 3 and maintaining an SH molarity of 16 led to a reduced w/b ratio, consequently optimizing the compressive strength, split tensile strength, and elastic modulus of the UHP-GC specimen. This observation underscores the impact of alkaline activation and SH molarity on the resilience of UHP-GC. A high alkalinity of the UHP-GC mixture is imperative for expediting the dissolution of silica and alumina during the conversion of aluminosilicate raw materials into a robust three-dimensional geopolymer network within the UHP-GC matrix.

- The microstructures of UHP-GC specimens detailed in numerous published studies reveal densely packed surfaces characterized by minimally identifiable pores. UHP-GC samples based on GGBS exhibited semi-crystalline microstructures, whereas those UHP-GC samples enriched with higher proportions of silica and alumina in their precursors showed amorphous microstructures. The XRD analysis of the UHP-GC samples revealed traces of minerals linked to N-A-S-H and C-A-S-H gels, including akermanite, mullite, gismondine, gehlenite, albite, microcline, nepheline, and alite. The presence of these minerals within the UHP-GC samples corroborates that their bonding performance was intricately governed by the judicious selection and proportioning of alkaline activators and precursors.

Aside from the raw materials examined in this review, it is recommendable for forthcoming research endeavors to investigate alternative waste-derived constituents suitable for the advancement of UHP-GC. In consideration of this, industrial waste like lime sludge, also classified as an alkali waste, holds promising potential as an alkaline activator for UHP-GC. Furthermore, the utilization of sewage sludge ash, sawdust ash, and biochar, all derived from waste sources, presents an opportunity to serve as precursors for UHP-GC. These waste-originating raw materials, combined with recycled steel fibers, offer a viable avenue for sustainable investigation into the production of UHP-GC, aligning with the principles of the 'Waste-to-Wealth' paradigm. Waste-converted-to-wealth essentially denotes the transformation of waste from a state of depleted usefulness to a point of significant value and desirability.

6. Declarations

6.1. Author Contributions

Conceptualization, M.A.K.M.; validation, L.S.W.; formal analysis, M.A.K.M. and L.S.W.; investigation, M.A.K.M.; writing—original draft preparation, M.A.K.M. and L.S.W.; writing—review and editing, L.S.W., A.M.A.N.A., A.M.D.A.J., and S.C.P.; supervision, L.S.W. and A.M.A.N.A.; funding acquisition, M.A.K.M. All authors have read and agreed to the published version of the manuscript.

6.2. Data Availability Statement

Data sharing is not applicable to this article.

6.3. Funding

6.4. Acknowledgements

None.

6.5. Conflicts of Interest

The authors declare no conflict of interest.

7. References

[1] Ahmed, H. U., Mohammed, A. A., Rafiq, S., Mohammed, A. S., Mosavi, A., Sor, N. H., & Qaidi, S. M. A. (2021). Compressive strength of sustainable geopolymer concrete composites: A state-of-the-art review. Sustainability (Switzerland), 13(24), 13502. doi:10.3390/su132413502.

[2] Qaidi, S. M. A., Tayeh, B. A., Zeyad, A. M., de Azevedo, A. R. G., Ahmed, H. U., & Emad, W. (2022). Recycling of mine tailings for the geopolymers production: A systematic review. Case Studies in Construction Materials, 16, 933. doi:10.1016/j.cscm.2022.e00933.

[3] Li, N., Shi, C., Wang, Q., Zhang, Z., & Ou, Z. (2017). Composition design and performance of alkali-activated cements. Materials and Structures/Materiaux et Constructions, 50(3), 1–11. doi:10.1617/s11527-017-1048-0.

[4] Nuaklong, P., Sata, V., & Chindaprasirt, P. (2018). Properties of metakaolin-high calcium fly ash geopolymer concrete containing recycled aggregate from crushed concrete specimens. Construction and Building Materials, 161, 365–373. doi:10.1016/j.conbuildmat.2017.11.152.

[5] Zhang, Z., Provis, J. L., Reid, A., & Wang, H. (2014). Fly ash-based geopolymers: The relationship between composition, pore structure and efflorescence. Cement and Concrete Research, 64, 30–41. doi:10.1016/j.cemconres.2014.06.004.

[6] Shaikh, F. U. A. (2016). Mechanical and durability properties of fly ash geopolymer concrete containing recycled coarse aggregates. International Journal of Sustainable Built Environment, 5(2), 277–287. doi:10.1016/j.ijsbe.2016.05.009.

[7] Rajini, B., & Sashidhar, C. (2019). Prediction mechanical properties of GGBS based on geopolymer concrete by using analytical method. Materials Today: Proceedings, 19, 536–540. doi:10.1016/j.matpr.2019.07.729.

[8] Parashar, A. K., Sharma, P., & Sharma, N. (2022). Effect on the strength of GGBS and fly ash based geopolymer concrete. Materials Today: Proceedings, 62, 4130–4133. doi:10.1016/j.matpr.2022.04.662.

[9] Mejía, J. M., Mejía de Gutiérrez, R., & Puertas, F. (2013). Rice husk ash as a source of silica in alkali-activated fly ash and slag cementitious systems. Construction Materials, 63(311), 361–375. doi:10.3989/mc.2013.04712.

[10] Phoo-Ngernkham, T., Maegawa, A., Mishima, N., Hatanaka, S., & Chindaprasirt, P. (2015). Effects of sodium hydroxide and sodium silicate solutions on compressive and shear bond strengths of FA-GBFS geopolymer. Construction and Building Materials, 91, 1–8. doi:10.1016/j.conbuildmat.2015.05.001.

[11] Smirnova, O. M. (2018). Technology of increase of nanoscale pores volume in protective cement matrix. International Journal of Civil Engineering and Technology, 9(10), 1991–2000.

[12] Shi, C., Qu, B., & Provis, J. L. (2019). Recent progress in low-carbon binders. Cement and Concrete Research, 122, 227–250. doi:10.1016/j.cemconres.2019.05.009.

[13] Ahmed, H. U., Mohammed, A. S., Qaidi, S. M. A., Faraj, R. H., Hamah Sor, N., & Mohammed, A. A. (2023). Compressive strength of geopolymer concrete composites: a systematic comprehensive review, analysis and modeling. European Journal of Environmental and Civil Engineering, 27(3), 1383–1428. doi:10.1080/19648189.2022.2083022.

[14] Ahmed, H. U., Mohammed, A. S., Faraj, R. H., Qaidi, S. M. A., & Mohammed, A. A. (2022). Compressive strength of geopolymer concrete modified with nano-silica: Experimental and modeling investigations. Case Studies in Construction Materials, 16, 1036. doi:10.1016/j.cscm.2022.e01036.

[15] Liu, Y., Shi, C., Zhang, Z., Li, N., & Shi, D. (2020). Mechanical and fracture properties of ultra-high performance geopolymer concrete: Effects of steel fiber and silica fume. Cement and Concrete Composites, 112, 103665. doi:10.1016/j.cemconcomp.2020.103665.

[16] Ambily, P. S., Ravisankar, K., Umarani, C., Dattatreya, J. K., & Iyer, N. R. (2014). Development of ultra-high-performance geopolymer concrete. Magazine of Concrete Research, 66(2), 82–89. doi:10.1680/macr.13.00057.

[17] Mansour, W., & Tayeh, B. A. (2020). Shear Behaviour of RC Beams Strengthened by Various Ultrahigh Performance Fibre-Reinforced Concrete Systems. Advances in Civil Engineering, 2020, 1–18. doi:10.1155/2020/2139054.

[18] Bahmani, H., Mostofinejad, D., & Ali Dadvar, S. (2020). Mechanical properties of ultra-high-performance fiber- reinforced concrete containing synthetic and mineral fibers. ACI Materials Journal, 117(3), 155–168. doi:10.14359/51724596.

[19] Bahmani, H., Mostofinejad, D., & Dadvar, S. A. (2020). Effects of Synthetic Fibers and Different Levels of Partial Cement Replacement on Mechanical Properties of UHPFRC. Journal of Materials in Civil Engineering, 32(12), 4020361. doi:10.1061/(asce)mt.1943-5533.0003462.

[20] Bahmani, H., Mostofinejad, D., & Dadvar, S. A. (2022). Fiber Type and Curing Environment Effects on the Mechanical Performance of UHPFRC Containing Zeolite. Iranian Journal of Science and Technology, Transactions of Civil Engineering, 46(6), 4151–4167. doi:10.1007/s40996-022-00911-z.

[21] Bahmani, H., & Mostofinejad, D. (2022). Microstructure of ultra-high-performance concrete (UHPC) – A review study. Journal of Building Engineering, 50, 104118. doi:10.1016/j.jobe.2022.104118.

[22] Leng, Y., Rui, Y., Zhonghe, S., Dingqiang, F., Jinnan, W., Yonghuan, Y., Qiqing, L., & Xiang, H. (2023). Development of an environmental Ultra-High Performance Concrete (UHPC) incorporating carbonated recycled coarse aggregate. Construction and Building Materials, 362, 129657. doi:10.1016/j.conbuildmat.2022.129657.

[23] Liu, K., Yin, T., Fan, D., Wang, J., & Yu, R. (2022). Multiple effects of particle size distribution modulus (q) and maximum aggregate size (Dmax) on the characteristics of Ultra-High Performance concrete (UHPC): Experiments and modeling. Cement and Concrete Composites, 133, 104709. doi:10.1016/j.cemconcomp.2022.104709.

[24] Qaidi, S. M. A., Sulaiman Atrushi, D., Mohammed, A. S., Unis Ahmed, H., Faraj, R. H., Emad, W., Tayeh, B. A., & Mohammed Najm, H. (2022). Ultra-high-performance geopolymer concrete: A review. Construction and Building Materials, 346, 128495. doi:10.1016/j.conbuildmat.2022.128495.

[25] Sun, M., Yu, R., Jiang, C., Fan, D., & Shui, Z. (2022). Quantitative effect of seawater on the hydration kinetics and microstructure development of Ultra High Performance Concrete (UHPC). Construction and Building Materials, 340, 127733. doi:10.1016/j.conbuildmat.2022.127733.

[26] Samuvel Raj, R., Prince Arulraj, G., Anand, N., Kanagaraj, B., Lubloy, E., & Naser, M. Z. (2023). Nanomaterials in geopolymer composites: A review. Developments in the Built Environment, 13, 100114. doi:10.1016/j.dibe.2022.100114.

[27] Dheyaaldin, M. H., Mosaberpanah, M. A., Shi, J., & alzeebaree, R. (2023). The effects of nanomaterials on the characteristics of aluminosilicate-based geopolymer composites: A critical review. Journal of Building Engineering, 73, 106713. doi:10.1016/j.jobe.2023.106713.

[28] Swathi, B., & Vidjeapriya, R. (2023). Influence of precursor materials and molar ratios on normal, high, and ultra-high performance geopolymer concrete – A state of art review. Construction and Building Materials, 392, 132006. doi:10.1016/j.conbuildmat.2023.132006.

[29] Lao, J. C., Huang, B. T., Fang, Y., Xu, L. Y., Dai, J. G., & Shah, S. P. (2023). Strain-hardening alkali-activated fly ash/slag composites with ultra-high compressive strength and ultra-high tensile ductility. Cement and Concrete Research, 165, 107075. doi:10.1016/j.cemconres.2022.107075.

[30] Liu, Y., Zhang, Z., Shi, C., Zhu, D., Li, N., & Deng, Y. (2020). Development of ultra-high performance geopolymer concrete (UHPGC): Influence of steel fiber on mechanical properties. Cement and Concrete Composites, 112, 103670. doi:10.1016/j.cemconcomp.2020.103670.

[31] Aisheh, Y. I. A., Atrushi, D. S., Akeed, M. H., Qaidi, S., & Tayeh, B. A. (2022). Influence of steel fibers and microsilica on the mechanical properties of ultra-high-performance geopolymer concrete (UHP-GPC). Case Studies in Construction Materials, 17, 1245. doi:10.1016/j.cscm.2022.e01245.

[32] Tayeh, B. A., Akeed, M. H., Qaidi, S., & Bakar, B. H. A. (2022). Influence of microsilica and polypropylene fibers on the fresh and mechanical properties of ultra-high performance geopolymer concrete (UHP-GPC). Case Studies in Construction Materials, 17, 1367. doi:10.1016/j.cscm.2022.e01367.

[33] Tahwia, A. M., Heniegal, A. M., Abdellatief, M., Tayeh, B. A., & Elrahman, M. A. (2022). Properties of ultra-high performance geopolymer concrete incorporating recycled waste glass. Case Studies in Construction Materials, 17, 1393. doi:10.1016/j.cscm.2022.e01393.

[34] Unis Ahmed, H., Mahmood, L. J., Muhammad, M. A., Faraj, R. H., Qaidi, S. M. A., Hamah Sor, N., Mohammed, A. S., & Mohammed, A. A. (2022). Geopolymer concrete as a cleaner construction material: An overview on materials and structural performances. Cleaner Materials, 5, 100111. doi:10.1016/j.clema.2022.100111.

[35] Wang, F., Sun, X., Tao, Z., & Pan, Z. (2022). Effect of silica fume on compressive strength of ultra-high-performance concrete made of calcium aluminate cement/fly ash based geopolymer. Journal of Building Engineering, 62, 105398. doi:10.1016/j.jobe.2022.105398.

[36] Kathirvel, P., & Sreekumaran, S. (2021). Sustainable development of ultra-high performance concrete using geopolymer technology. Journal of Building Engineering, 39, 102267. doi:10.1016/j.jobe.2021.102267.

[37] Yoo, D. Y., & Banthia, N. (2016). Mechanical properties of ultra-high-performance fiber-reinforced concrete: A review. Cement and Concrete Composites, 73, 267–280. doi:10.1016/j.cemconcomp.2016.08.001.

[38] Yoo, D. Y., Kang, S. T., & Yoon, Y. S. (2014). Effect of fiber length and placement method on flexural behavior, tension-softening curve, and fiber distribution characteristics of UHPFRC. Construction and Building Materials, 64, 67–81. doi:10.1016/j.conbuildmat.2014.04.007.

[39] Aydin, S., & Baradan, B. (2013). The effect of fiber properties on high performance alkali-activated slag/silica fume mortars. Composites Part B: Engineering, 45(1), 63–69. doi:10.1016/j.compositesb.2012.09.080.

[40] Aisheh, Y. I. A., Atrushi, D. S., Akeed, M. H., Qaidi, S., & Tayeh, B. A. (2022). Influence of polypropylene and steel fibers on the mechanical properties of ultra-high-performance fiber-reinforced geopolymer concrete. Case Studies in Construction Materials, 17, 1234. doi:10.1016/j.cscm.2022.e01234.

[41] Yoo, D. Y., Lee, J. H., & Yoon, Y. S. (2013). Effect of fiber content on mechanical and fracture properties of ultra-high performance fiber reinforced cementitious composites. Composite Structures, 106, 742–753. doi:10.1016/j.compstruct.2013.07.033.

[42] Guo, X., & Pan, X. (2018). Mechanical properties and mechanisms of fiber reinforced fly ash–steel slag based geopolymer mortar. Construction and Building Materials, 179, 633–641. doi:10.1016/j.conbuildmat.2018.05.198.

[43] Lao, J. C., Xu, L. Y., Huang, B. T., Dai, J. G., & Shah, S. P. (2022). Strain-hardening Ultra-High-Performance Geopolymer Concrete (UHPGC): Matrix design and effect of steel fibers. Composites Communications, 30, 101081. doi:10.1016/j.coco.2022.101081.

[44] Mousavinejad, S. H. G., & Sammak, M. (2022). An assessment of the fracture parameters of ultra-high-performance fiber-reinforced geopolymer concrete (UHPFRGC): The application of work of fracture and size effect methods. Theoretical and Applied Fracture Mechanics, 117, 103157. doi:10.1016/j.tafmec.2021.103157.

[45] Liu, J., Wu, C., Li, J., Liu, Z., Xu, S., Liu, K., Su, Y., Fang, J., & Chen, G. (2021). Projectile impact resistance of fibre-reinforced geopolymer-based ultra-high performance concrete (G-UHPC). Construction and Building Materials, 290, 123189. doi:10.1016/j.conbuildmat.2021.123189.

[46] Mousavinejad, S. H. G., & Sammak, M. (2021). Strength and chloride ion penetration resistance of ultra-high-performance fiber reinforced geopolymer concrete. Structures, 32, 1420–1427. doi:10.1016/j.istruc.2021.03.112.

[47] Tahwia, A. M., Abd Ellatief, M., Heneigel, A. M., & Abd Elrahman, M. (2022). Characteristics of eco-friendly ultra-high-performance geopolymer concrete incorporating waste materials. Ceramics International, 48(14), 19662–19674. doi:10.1016/j.ceramint.2022.03.103.

[48] Tahwia, A. M., Ellatief, M. A., Bassioni, G., Heniegal, A. M., & Elrahman, M. A. (2023). Influence of high temperature exposure on compressive strength and microstructure of ultra-high performance geopolymer concrete with waste glass and ceramic. Journal of Materials Research and Technology, 23, 5681–5697. doi:10.1016/j.jmrt.2023.02.177.

[49] Liu, J., Wu, C., Liu, Z., Li, J., Xu, S., Liu, K., Su, Y., & Chen, G. (2021). Investigations on the response of ceramic ball aggregated and steel fibre reinforced geopolymer-based ultra-high performance concrete (G-UHPC) to projectile penetration. Composite Structures, 255, 112983. doi:10.1016/j.compstruct.2020.112983.

[50] Mousavinejad, S. H. G., & Sammak, M. (2022). An assessment of the effect of Na_2SiO_3/NaOH ratio, NaOH solution concentration, and aging on the fracture properties of ultra-high-performance geopolymer concrete: The application of the work of fracture and size effect methods. Structures, 39, 434–443. doi:10.1016/j.istruc.2022.03.045.

[51] Sathonsaowaphak, A., Chindaprasirt, P., & Pimraksa, K. (2009). Workability and strength of lignite bottom ash geopolymer mortar. Journal of Hazardous Materials, 168(1), 44–50. doi:10.1016/j.jhazmat.2009.01.120.

[52] Rattanasak, U., & Chindaprasirt, P. (2009). Influence of NaOH solution on the synthesis of fly ash geopolymer. Minerals Engineering, 22(12), 1073–1078. doi:10.1016/j.mineng.2009.03.022.

[53] Elyamany, H. E., Abd Elmoaty, A. E. M., & Elshaboury, A. M. (2018). Setting time and 7-day strength of geopolymer mortar with various binders. Construction and Building Materials, 187, 974–983. doi:10.1016/j.conbuildmat.2018.08.025.

[54] Lao, J. C., Xu, L. Y., Huang, B. T., Zhu, J. X., Khan, M., & Dai, J. G. (2023). Utilization of sodium carbonate activator in strain-hardening ultra-high-performance geopolymer concrete (SH-UHPGC). Frontiers in Materials, 10. doi:10.3389/fmats.2023.1142237.

[55] Bahmani, H., & Mostofinejad, D. (2023). A review of engineering properties of ultra-high-performance geopolymer concrete. Developments in the Built Environment, 14, 100126. doi:10.1016/j.dibe.2023.100126.

[56] Alharbi, Y. R., Abadel, A. A., Salah, A. A., Mayhoub, O. A., & Kohail, M. (2021). Engineering properties of alkali activated materials reactive powder concrete. Construction and Building Materials, 271, 121550. doi:10.1016/j.conbuildmat.2020.121550.

[57] Ng, C., Alengaram, U. J., Wong, L. S., Mo, K. H., Jumaat, M. Z., & Ramesh, S. (2018). A review on microstructural study and compressive strength of geopolymer mortar, paste and concrete. Construction and Building Materials, 186, 550–576. doi:10.1016/j.conbuildmat.2018.07.075.

[58] Aydin, S., & Baradan, B. (2013). Engineering properties of reactive powder concrete without portland cement. ACI Materials Journal, 110(6), 619–627. doi:10.14359/51686329.

[59] Mehta, A., & Siddique, R. (2017). Strength, permeability and micro-structural characteristics of low-calcium fly ash based geopolymers. Construction and Building Materials, 141, 325–334. doi:10.1016/j.conbuildmat.2017.03.031.

[60] Wong, L. S., Oweida, A. F. M., Kong, S. Y., Iqbal, D. M., & Regunathan, P. (2020). The surface coating mechanism of polluted concrete by Candida ethanolica induced calcium carbonate mineralization. Construction and Building Materials, 257, 119482. doi:10.1016/j.conbuildmat.2020.119482.

[61] Duan, P., Yan, C., & Zhou, W. (2017). Compressive strength and microstructure of fly ash based geopolymer blended with silica fume under thermal cycle. Cement and Concrete Composites, 78, 108–119. doi:10.1016/j.cemconcomp.2017.01.009.

[62] López, A. H., Calvo, J. L. G., Olmo, J. G., Petit, S., & Alonso, M. C. (2008). Microstructural evolution of calcium aluminate cements hydration with silica fume and fly ash additions by scanning electron microscopy, and mid and near-infrared spectroscopy. Journal of the American Ceramic Society, 91(4), 1258–1265. doi:10.1111/j.1551-2916.2008.02283.x.

[63] Vafaei, M., & Allahverdi, A. (2016). Influence of calcium aluminate cement on geopolymerization of natural pozzolan. Construction and Building Materials, 114, 290–296. doi:10.1016/j.conbuildmat.2016.03.204.

[64] Wong, L. S. (2022). Durability Performance of Geopolymer Concrete: A Review. Polymers, 14(5), 868. doi:10.3390/polym14050868.